INSTITUTO POLITÉCNICO DE BRAGANÇA

FIRE RESISTANCE OF PROTECTED AND UNPROTECTED CELLULAR BEAMS

Lamri Brahim

Final thesis presented to

SCHOOL OF TECHNOLOGY AND MANAGEMENT

POLYTECHNIC INSTITUTE OF BRAGANÇA

For the fulfilment of the Master Degree in

CONSTRUCTION ENGINEERING

July, 2016

FIRE RESISTANCE OF PROTECTED AND UNPROTECTED CELLULAR BEAMS

Lamri Brahim

Final thesis submitted to the

School of Technology and Management

Polytechnic Institute of Bragança

For the fulfilment of the Master Degree in

CONSTRUCTION ENGINEERING

Supervisor at IPB:

Prof Dr. Luis Mesquita

Supervisor at UHBC:

Prof Dr. Abdelhak Kada

July, 2016

ACKNOWLEDGMENTS:

I would like to thank my supervisor Dr. Luis Mesquita and Dr.Kada Abdelhak for giving me the opportunity to carry out research work related to the field of structural engineering and fire protection. I am highly indebted to his valuable thoughts and contributions towards the development of my thesis and also for providing me with an sample amount of knowledge about the field of fire protection engineering.

I would also like to thank the entire laboratory assistants for their guidelines and support as a senior to help me carry out appropriate research strategies for facilitating this thesis project.

My special thanks to all the other staff members at the Civil Engineering of Polytechnic Institute of Bragança whose contributions and supports have been invaluable.

I would like to deliver my thankfulness to acknowledge the help given by teachers, and friends who involved directly or indirectly to the success of this thesis.

Finally, thanks to my familly for encouragement, love, guidance and support needed to complete this thesis.

Resumo

As vigas alveolares são vigas de aço estruturais que são mais profundas do que as secções laminadas convencionais com furos localizados na alma. Como o modo de colapso por encurvadura local da alma pode ocorrer antes da secção atingir a temperatura limite, normalmente é necessário um aumento do material de proteção dos elementos com aberturas na alma em comparação com as secções sólidas equivalentes. Verificando-se que a temperatura do aço da alma entre as furações é superior à temperatura das vigas sólidas motivou a realização de ensaios experimentais ao fogo. Estes ensaios foram maioritariamente realizados pelos fabricantes de tintas intumescentes devido à necessidade de fornecerem as suas próprias tabelas de espessuras, e os resultados mantidos confidenciais.

A espessura de tinta intumescente requerida para fornecer a capacidade de resistência ao fogo definida regulamentarmente de uma viga alveolar depende da espessura da alma, das dimensões e forma das furações, da largura da alma entre furações (*web post*), do grau de utilização da seção e da eficiência de proteção da tinta intumescente. A avaliação de desempenho das tintas intumescentes aplicadas a vigas alveolares requer uma análise elementar da temperatura, da alma e dos banzos, considerando os resultados dos testes em vigas sólidas segundo a EN 13381-8. Estes resultados definem uma linha base que é complementada com os resultados de testes de resistência ao fogo de vigas alveolares, segundo a EN 13381-9, que permitem a avaliação de desempenho em função da largura da alma entre furações (web posts) e o fator de massividade da secção.

Este trabalho apresenta uma investigação relativa ao comportamento de vigas alveolares em condições de incêndio com e sem materiais de proteção ao fogo. São analisadas vigas com diferentes geométricas ao nível do diâmetro da furação espassamento da furação e da espessura do material de proteção ao fogo. Estes ensaios de resistência ao fogo são ainda comparados ao nível da evolução da temperaura do aço com os resultados provenientes de vigas sólidas de perfis laminados com e sem proteção ao fogo. Os resultados experimentais da evolução da temperatura permite a análise da eficiência da tinta intumescente na proteção ao fogo de vigas alveolares em comparação com as vigas alveolares sem proteção e com as vigas sólidas.

Palavas-chave: Tinta intumescente; Resistência ao fogo; Proteção ao fogo; Vigas alveolares; Testes Experimentais

Abstract

Cellular beams are structural steel beams that are deeper than normal rolled sections and have holes cut into their webs. As the web post failure may occur before the section reaches the limiting temperature usually an increase in the fire protection may be required for members with web openings in comparison to its equivalent solid section.

The questions raised about the temperature of the web post being higher than a similar solid beam motivated the need of further experimental fire tests. These were mainly conducted by the coatings manufactures due to their needs to supply their own loading tables, and its results were kept confidential.

It is recognised that the intumescent fire protection thickness required to provide a given fire resistance to a cellular beam depends on its web thickness, the hole shape and dimensions, the width of the web post, the degree of the beam asymmetry and the structural utilisation factor, as well as the protection efficiency of the intumescent coating.The assessment method of cellular beams protected with intumescent coatings needs a multi-temperature analysis (MTA) of the coating assessment on solid beams, for each fire protection period, performed accordingly to EN 13381-8. The solid beam assessment provides a DFT baseline against which a suitable enhancement for cellular beams is added. Each fire test is carried out using five cellular beam sections, which enables a range of web post widths and section factors to be evaluated, instrumented with thermocouples around the holes, web post and bottom flange, as standardized in EN 13381-9.

The present study aims to investigate the behaviour of cellular beams under fire conditions when considering unprotected and intumescent protected cellular steel beam. Experimental tests are conducted in IPB furnace in both cases with and without protection where about temperature profiles are produced and analysed. The behaviour of the intumescent fire protection with different properties and thickness is monitored in the

furnace tests and conclusions are made. The experimental temperature results show intumescent coating efficiency when applied to solid beams and also for cellular beams, resulting from its application an increase fire the resistance time in both cases.

Keywords: Intumescent coatings; Fire resistance; Fire protection; Cellular Beams, Experimental tests

Index

Liste of Figures

List of Tables

Simbology

$\Delta\theta a$	steel temperature increase from time t to time $t+\Delta t$
k_{sh}	correction factor for the shadow effect, see below
A_m	surface area of the member per unit length
V	volume of the member per unit length
c_a	specific heat of steel
ρ_a	unit mass of steel
$\dot{h}_{net}$	design value of the net heat flux per unit area
Δt	time interval
λ_p	thermal conductivity of the fire protection material
A_p/V	section factor for steel members insulated by fire protection material
A_p	area of fire protection material per unit length of the member
V	volume of the member per unit length
$\theta_{g,t}$	ambient gas temperature at time t
$\theta_{a,t}$	steel temperature at time t
d_p	thickness of the fire protection material
c_a	temperature dependant specific heat of steel
ρ_a	unit mass of steel
Δt	time interval
$\Delta\theta_{g,t}$	increase of ambient gas temperature during the time interval _t
c_p	temperature independent specific heat of the fire protection material
ρ_p	unit mass of the fire protection material
h	Heigh of section.
b	Width of section.
tw	Thickness of web.

tf	Thickness of flange.
r	Radius.
A	Area of section.
nh	Number of holes.
D	Diameter of hole.
rh	Radius of hole.
Ah	Area of a hole.
Hp	Perimeter of a hole.

Chapter 1. Introduction

1.1 Context and motivation

During the last decades, remarkable progress has been made in understanding not only the parameters which influence the development of building fires, but also the behaviour of fire exposed structural materials and structures. In particular, for steel structures, this progress has resulted in the production of very detailed rules for the design and calculation of structural behaviour and load bearing capacity in fire.

This research is to perform a comparison of the temperature evolution of cellular beams with and without a fire protection material based on the results of experimental fire tests. The analysis should show whether the temperature increase in the web post is at a faster rate than expected on solid web sections. This analysis is to be used for the definition of the cellular beams collapse mode, either from the buckling of the web post, the Vierendeel bending or the flange compression. The use of cellular beams allows a new architectural expression. Structures are lightened and spans increased, pulling spaces together.

1.2 State of the art

The cellular beam has generally followed a simple design rule based on calculating the Section Factor from which the cellular section was manufactured and then increasing the required thickness by 20% from parent beams. The difference between temperatures in the bottom flange and web-post of the protected cellular beam with intumescent coating, the behaviour of char 'pull-back' seems to be dependent on the thickness and type of intumescent coating used, [1].

Colin Bailey found that for the unprotected cellular beam there was no increase in web-post temperatures, but for a protected cellular beam the web-post temperatures were

higher compared to the web temperatures of a solid beam. A test of a symmetrical cellular beam and identical solid beam within the same furnace and comparing between the two beams for temperature evolution , [1].

The published work of Bailey, [1] investigate the rate of temperature increase in the web post and -compare it with solid beams, a series of tests were conducted on unloaded, protected and unprotected cellular and solid beams. The furnace test that in the beams with no fire protection, the flange and web post temperatures of the cellular beams was slightly lower than the corresponding temperatures of the solid beams. It was also observed that the ratio of the web to flange temperature did not increase at a faster rate in the cellular beam compared to the solid beam, [1].

The tests consisted of an unprotected set of beams followed by 3 protected sets of beams, comprising one with 0.8 [mm] thick water-based intumescent, also two with 0,8 and 2,1 [mm] thick solvent-based intumescent.

Figure 1 shows the comparaison of average temperatures on the bottom flange of the cellular beam with average temperatures on the bottom flange of the solid beam. The solid beam is hotter than the cellular beam, [1].

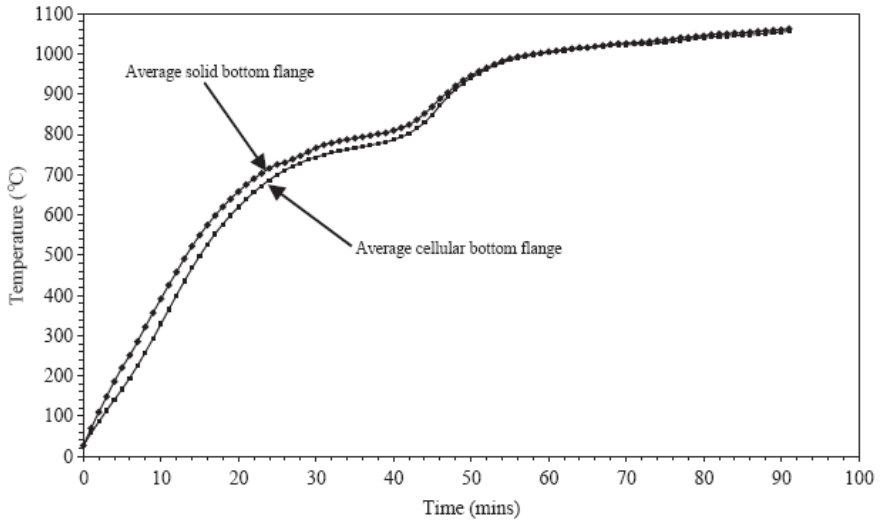

Figure 1 Comparison between recorded average temperatures on the bottom flange of the cellular beam with average temperatures on the bottom flange of the solid beam, [1].

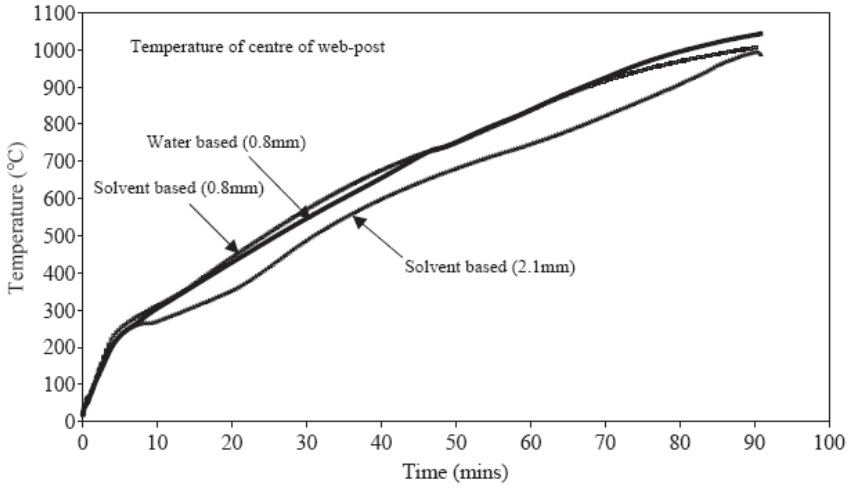

Figure 2 Comparison of temperatures at centre of web post for protected beams, [1]

Figure 2 shows that The beam protected with the 0.8mm water-based intumescent experienced higher web temperatures compared with 2.1mm solvent based and 0.8 solvent based, [1].

The test results of unprotected beams show that temperature of the web-post of a cellular beam was higher than the temperatures of an identical solid beam. However, the three tests on protected beams show that the temperatures measured within the web-post of a cellular beam were higher than the temperatures of the web for identical solid beam, [1].

The paper of Bihina and Bouchaïr [2] presented and used full-scale fire tests for analyse the behaviour of composite steel and concrete cellular beams with evenly spaced circular web holes and the test is to applied two-point mechanical load. The beams were not fire protected and they were tested with an ISO834 fire or a bilinear thermal curve representing the behaviour of a protected beam. Also the use of cellular beams, endowed with aesthetical and mechanical advantages requires a good understanding of their behaviour, at both ambient and elevated temperatures and the results that beams with slender web-posts and an asymmetrical steel cross-section were prone to fail by web-post buckling. On the other hand, beams with ‘‘reinforced’’ web-posts or large web-posts failed by flexural bending, like solid beams. At failure, the critical temperature could reach up to 500 [ºC] at slab mid-depth, and exceed 700 [ºC] in the steel web, [2].

The Web post buckling is the most relevant stability problem for the cellular beam. Wang study behaviour for protected cellular steel beams at elevated temperatures in a fire. Also they investigated and verify its behaviour by a finite element model. The partially protected steel beam represents a cellular steel beam (CSB) with the hole edge left unprotected. The temperature distribution in the web-post was non uniform, also for the

unprotected and fully protected CSB. The fire resistance time of cellular beam increased linearly with the increase of coating thickness. For the partially protected cellular steel beam, the temperature gradient in the web-post becomes higher with the increase in the fire protection thickness. With the increase in the fire protection thickness, the increment in the fire resistance time decreased. Additional thermal stress occurred due to the non-uniform thermal strain in the web-post. For the fully protected CSBs, the fire-resistance time increased linearly with increase in thecoating thickness. However, for the partially protected CSBs,with the increase in the fire protection thickness,the increment in the fire resistance time decreased., [3].

Figure 3 presents the temperature elevation point 1 and point 2 of the two kinds of protected CSBs. The temperature difference at point 1 and point 2 of the Cxx-1 was nearly the same which was about 60 °C.For the Cxx-2, the temperature difference at point1 and point 2 in web-posts increased with the increase in coating thickness,which were 136 °C, 183 °C, 221 °C and 240 °C, respectively. The difference in the fire resistance time was determined by the difference in temperature elevation of the CSBs with different fire coating thickness., [3].

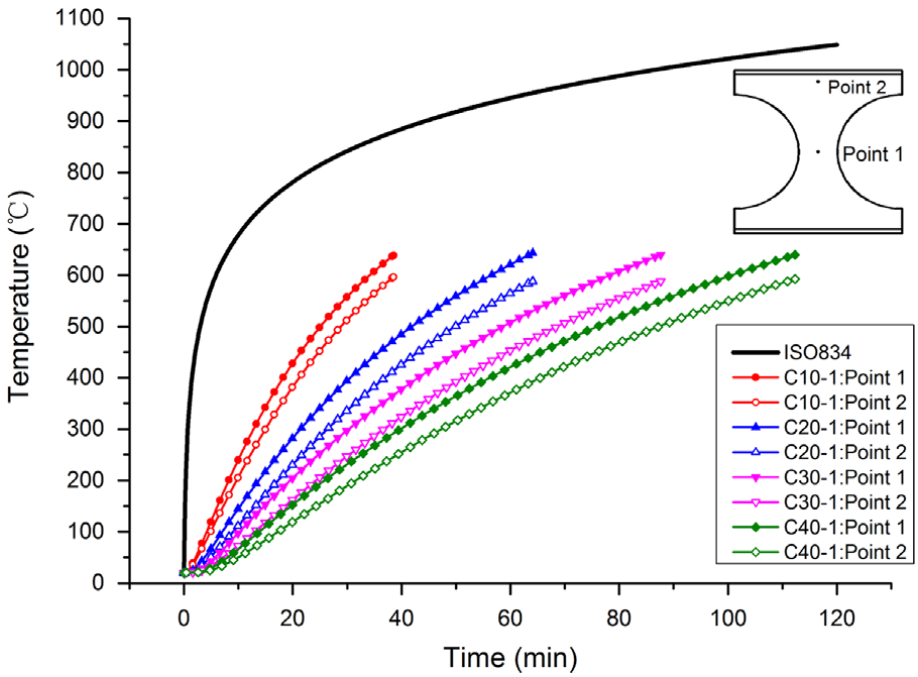

Figure 3 Temperature elevation of fully protected web-posts with different fire protection thickness., [3].

The temperature increment of unprotected and fully protected CSB in the web-post was non-uniform. For the CSB with load ratio of 0.5, the temperature difference in the web-post was about 60 °C at buckling. The temperature difference was much higher in the web-post of a partially protected CSB. In addition, the non-uniformity of temperature becomes greater with the increase in the fire protection thickness. The temperature distribution was non-uniform along both the section height and the longitudinal direction.For the fully protected CSBs, the fire-resistance time increased linearly with increase in the coating thickness. However, for the partially protected CSBs, with the increase in the fire protection thickness, the increment in the fire resistance time decreased., [3].

Guo-Qiang Li presents a study to investigate the feasibility of using a constant thermal conductivity for intumescent coating when calculating protected steel temperature in fire, based on analysing a series of fire tests on intumescent coating protected steel sections with a range of section factors and intumescent coating thicknesses. Having a constant thermal conductivity enables simplified analytical equations to be developed for design purpose, [4]. Their tests allow concluding that the effective constant thermal conductivity is a very simple concept and makes derivation of simple design equations possible. The research has demonstrated that it is feasible to use an effective constant thermal conductivity value to represent the temperature dependent thermal conductivity of intumescent coating, based on comparison of steel temperatures calculated using the effective constant thermal conductivity with the fire test results. The effective constant thermal conductivity tends to increase with decreasing rate of heating of steel (increasing DFT, decreasing section factor). The effective constant thermal conductivity changes with coating thickness and steel section factor. Therefore, it is necessary to obtainad at a base of effective constant thermal conductivity values for realistic applications with different DFTs and steel section factors. This research has indicated that it is possible to obtain this data base by conducting fire tests on steel plates, [4].

Nadjai et al conducted an experimental study at elevated temperatures on the behaviour of full-scale composite floor unprotected and protected cellular steel beams with intumescent coating having different size and openings shape. All beams were designed for full shear connections between the steel beam and the concrete flange using headed shear studs in order to fail in by web-post buckling. In fire, the temperature distribution across a composite member is non-uniform, since the web and bottom flange have thin cross-

sections and a large exposed perimeter than the top flange. The deterioration of the material properties of the web will therefore become an important effect on the overall performance of the member in the event of fire. Fire resistance and protection of cellular beams has been very controversial concerning their behaviour in elevated temperatures, the fire protection material and the required thickness, [5]. The tests were carried out on six full-scale composite unprotected and protected cellular beams, of 5 m span length. The cellular beams were fabricated from standard hot rolled steel sections, subjected to one or two point loads, using three different geometries and for fire protection of the cellular beams was used the intumescent coating material Nullfire S707-60, [5].

From the experimental tests of composite floor with protected and unprotected cellular steel beams in fire conditions conducted at the FireSERT, the authors concluded that the recorded temperatures on the protected steel sections are smaller than the unprotected. Also, the deformation of the protected composite cellular beams is less crucial than the unprotected. The failure mechanism in the three protected composite cellular beams is the same as the unprotected but with a longer duration time.

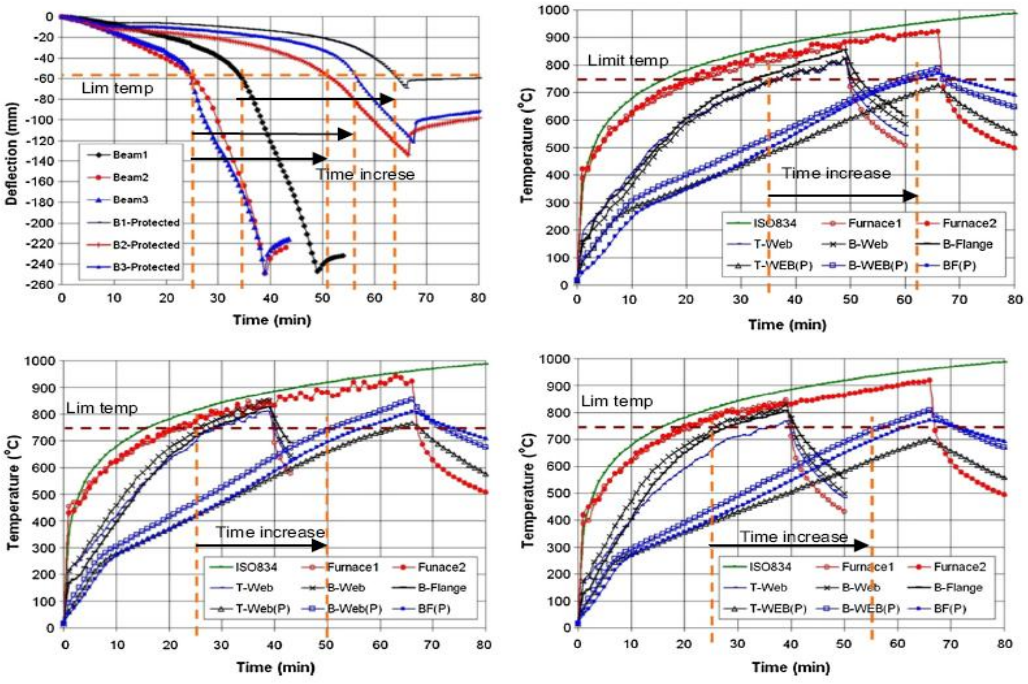

Figure 4 Deflections and temperatures distribution on protected and unprotected cellular beams, [5].

The composite cellular beams with protection failed in longer time than the unprotected and the recorded deflection at failure time was smaller than the unprotected. Temperature distribution and deflection results confirmed the effectiveness and importance

of applying fire protection on cellular beams. The results in protected beams showed in Figure 4 an increase of fire resistance of all protected beam up to 50% compared with unprotected beams when the temperature is 750 [ºC] for time limit of 60 [min] as provided by the manufacturer, [5].This research and the test results show that the intumescent coatings are the most effective fire protection material for steel cellular beams. The numerical model is capable of simulate the mechanical behaviour of composite cellular beam sections protected at elevated temperature conditions with a relatively high accuracy. The Eurocode provided equation used in DIANA can provide quite good agreement with the experimental results when it is calibrated with the correct material specification of the intumescent coating used. The simplicity and versatility of the Eurocode with more additional data can be an attractive for application in fire resistance assessment in design, [5].

The use of adequate edge concordance radius in beams with rectangular and square openings is very efficient for better distributing steel beam web stresses since it reduces the stress concentration at these points. Using an edge concordance radius equal to five times the web thickness in a six meter span beam (IPE750x137) with a rectangular opening height equal to 0.5 H increased in 9% its ultimate load, [6].

The beams with rectangular openings presented the smaller ultimate loads, about 30% less than their equivalent beams with square or circular openings. In these specimens the Vierendeel collapse mechanism was observed in all beams with rectangular openings and was independent of the beam opening position on the span. Beams with square openings presented a collapse mode combining the Vierendeel collapse mechanism with a load application point bending collapse, [7].

Research on the performance of beams with multiple web openings was seriously followed in 1964 when Kolosowski tested one castellated beam to study its deflection and failure mode. The overall height of this beam was 150% of its parent section, the span to depth ratio was 10 and the web post had the angle of 56.3° (this angle is 60° in UK sections). Kolosowski was expecting a behaviour similar to a Vierendeel truss, however, the beam eventually failed due to overall lateral torsional buckling as there were no lateral restraints provided within the supports. In 1973, Husain and Speirs conducted twelve tests to investigate the effect of the opening geometry on the mode of failure of these beams. In their tests they observed three different failure types, flexural failure, Vierendeel failure and web post buckling.

The web post buckling was only known as a major failure of such beams since 1996 when Zaarour and Redwood tested 12 short span (3000 mm) castellated beams with thin webs with minimum web post width to opening depth ratio ranging from 0.18 to 0.26. Most of these beams failed due to web post buckling and the rest failed due to lateral-torsional buckling. Redwood and Demirdjian also focused more on the web post buckling and tested four short span castellated beams with the UK cutting details. In his tests, he observed a double deviation web post bukling of 12 tests but for the longest beam he view a single deviation in the web post. The test results showed that web post buckling loads were not sensitive to the moment/shear ratio, [7].

The rate of increase in temperature of a steel cross-section is determined by the ratio of the heated surface area (A) to the volume (V). This ratio, A/V, has units of [m^{-1}] and is known as the "Section Factor". Members with low Section Factors will heat up more slowly.

In earlier editions of this publication the Section Factor was written as Hp/A. In the new European testing and design standards (ENV13381-4, ENV1993-1-2 and ENV1994-1-2) the Section Factor is presented as A/V, which has the same numerical value as Hp/A. It is likely that the designation Hp/A will gradually fall into disuse, [8].

A steel section with a large surface area (A) will receive more heat than one with a smaller surface area. Also, the greater the volume (V) of the section, the greater is the heat sink. It follows therefore, that a small thick section will increase its temperature slower than a large thin one. The Section Factor (A/V) is thus a measure of the rate at which a section will heat up in a fire and the higher its value the greater will be the protection thickness required, [8].

The lateral torsional buckling behaviour of cellular beams was investigated using a numerical model that was validated based on experimental results. The effect of the modified residual stress pattern was appropriately taken into account. Using the results of the parametric study, a preliminary design approach was proposed. This approach is based on the currently existing European guidelines for the calculation of the lateral torsional buckling resistance of I-section beams, but with a modified calculation of the cross-sectional properties and a modified buckling curve selection, [9].

The lateral torsional buckling behaviour of cellular members subjected to a constant bending moment was analysed by Bake, considering the effect of the modified residual

stress pattern caused by the production procedure. A numerical model, validated by comparing it with experimental results, was used to study the lateral torsional buckling behaviour of a large variety of cellular beam geometries. Both the elastic critical buckling moment Mcr and the LTB resistance M_{Rd} were determined, and a preliminary design rule was proposed for both moment values, [9].

Figure 5: Lateral torsional buckling failure of a cellular member loaded by a bending, [9].

The tests done with Delphine Snoke were failed by lateral torsional buckling, without any perceivable local buckling effects. For most of the longer geometries, the load-deflection diagram kept increasing past the critical LTB moment, due to the stabilising effect of the considerable pre-buckling deformations. Since no value of numerical resistance moment by programme of abaqus MRd,abq could be determined for these cases, the corresponding results were not taken into account, [9].

The evenly spaced circular web openings in I-section cellular beams have an advantageous effect on the material used if these beams are loaded in strong-axis bending. However, not all aspects of the behaviour of such beams have been studied adequately, such as the lateral torsional buckling failure, [9]. Furthermore, the detrimental effect of the modification of the residual stresses by the production process, demonstrated by the authors, was never taken into account.

An experimental study of unloaded solid and cellular beams with circular holes in fire conditions with and without intumescent fire protection was done by Mesquita et al, [10]. These preliminary tests are the basis for generating an elemental multi-temperature analysis (EMTA) needed to assess cellular beams with intumescent protection as prescribed by the EN13381- 9. The tests were done on protected and unprotected solid and cellular beams subjected to a fire exposure on three sides and compared the performance of an intumescent coating as a fire protection material using beams with and without intumescent protection, [10].

Also the experimental tests were carried out with reference to the standards EN 13381-8 for solid beams protected with intumescent paint and EN13381-9 for the analysis of cellular beams protected with intumescent paint. The results of the tests show the intumescent coating efficiency when applied to solid beams and also for cellular beams, resulting from its application an increase in the fire resistance time in both cases. From the results of these tests the study is being extended to a wider parametric analysis considering different cellular beams geometries and intumescent coatings thicknesses to allow for a general elemental multi-temperature analysis (EMTA), [10].

Chapter 2: Standard fire resistance design of celular beams

2.1 Introduction

Cellular beams give architectural flexibility having open large spaces forming compartments, as it is possible to achieve long spans. This structural element is currently being widely commercial used, in multi-storey buildings and industrial buildings, warehouses and portal frames. The investigation of the behaviour of cellular beams at hight temperature is being done from the theoretical, experimental and numerical perspetives.

There are a lot of different failure modes that has been observed. In fire, the degradation of strength and stiffness of unprotected steel sections exposed to elevated temperatures can result to early structural colapse. The fire resistance of cellular beams has been very controversial in the recent years, considering the fire protection material and the required thickness in a number of guidelines documents published by the Steel Construction Institute, [5]. The most common fire protection material used for cellular beams is the intumescent coating, giving the advantage of allowing the passage of technical services as it can be applied without blocking the holes in the web. Intumescent coating is applied on steel structural elements at specific thickness, necessary to protect the structural element, minimising the wastage and hence cost. They can be applied in the fabricator's shop or on the completed structure on the construction site. The use of intumescent coating extends the loadbearing capacity of the steel structure. The stability of a building, having intumescent coating protected for structures or buildings in case of fire depends on the thickness of the coating, the depth and insulation properties.

2.2 Safety verification for load, time or temperature domains

The stability analysis can be performed through different approaches mentioned in the Eurocode: namely in the time domain, in the load domain and, in some cases, in the

temperature domain. These possibilities are illustrated on Figure 6 and Figure 7 for a simple case in which the applied load, the effect of action $E_{fi,d}$, is constant during the fire and the element is characterised by a single temperature, $\theta_{structure}$. The figures refer to the case of a nominal fire in which the fire temperature, θ_{fire}, is continuously increasing. The temperatures in the structure, $\theta_{structure}$, will therefore also be a continuously increasing as a function of time and, although this will not be demonstrated theoretically, it will be assumed that this induces a continuously decreasing load bearing capacity, $R_{fi,d,t}$, [11].

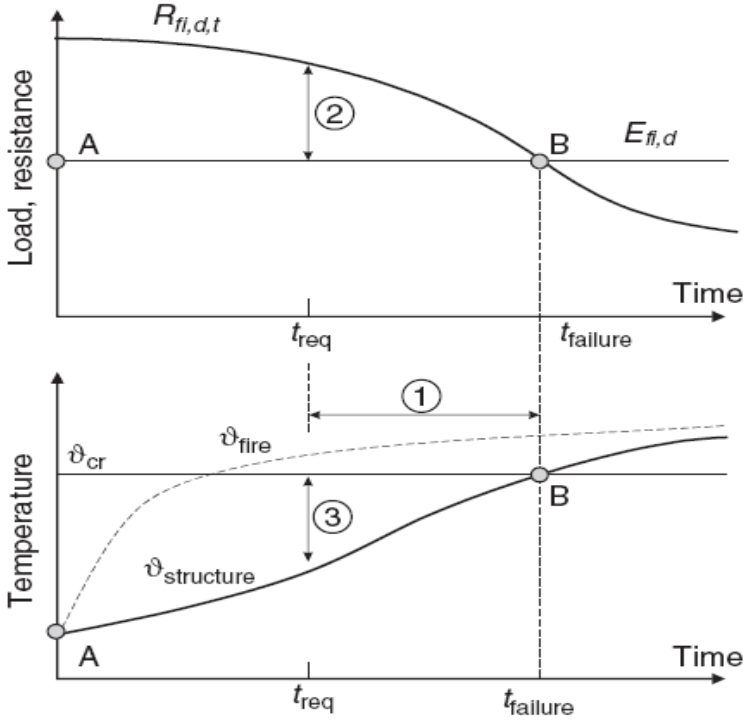

Figure 6: Load, time or temperature domain for a nominal fire, [11].

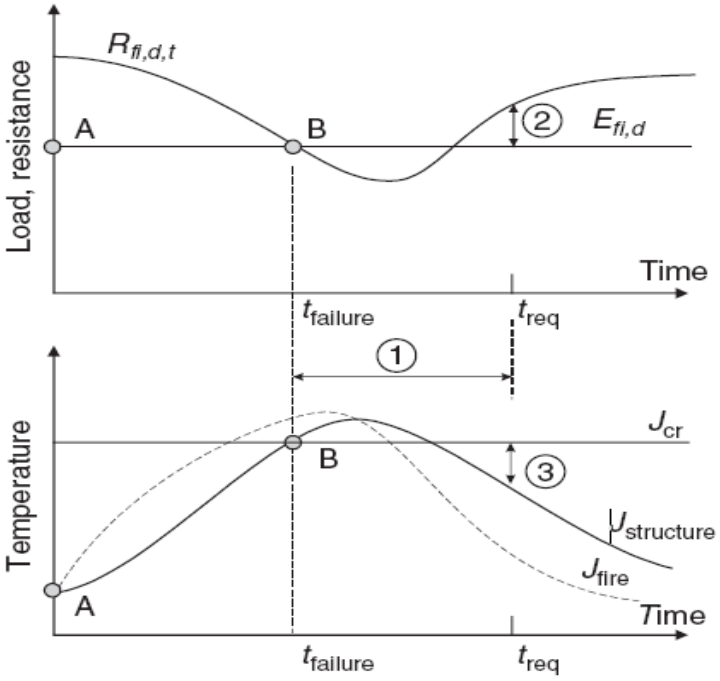

Figure 7: Load, time or temperature domain for a natural fire, [11].

For steel structures, the load bearing capacity of the structure that could be calculated at different moments in time produces a pattern as shown on Figure 7with a first phase where the load bearing capacity decreases as a function of time, and a second phase when the structure recovers its load bearing capacity, mainly because steel recovers its strength, either totally or partially, when cooling down to ambient temperature.

In each case, t_{req} noted on the Figure 7 is the required fire resistance time of the structure.

The situation at the beginning of the fire is represented by point A on both Figures and, if the analysis is performed by the advanced calculation model, the method, i.e. the software, normally will track the evolution of the situation of the structure until point B when failure occurs (most computer software indeed perform a transient step by step analysis). This means that the curve showing the evolution of the load bearing capacity is not known to the designer, [11].

2.2.1 Safety verification in time domain

It has to be verified that the time of failure $t_{failure}$ is higher than the required fire resistance time $t$req. This is expressed by Equation (1) and corresponds to the verification 1, satisfied on Figure 6 but not satisfied on Figure 7.

$$t_{failure} \geq t_{req} \tag{1}$$

2.2.2 Safety verification in load domain

At the required time in the fire t_{req}, it is verified that the resistance of the structure $R_{fi,d,t}$ is still higher than the effect of action $E_{fi,d}$. This is expressed by equation (2) and corresponds to the verification 2 on Figure 6 and Figure 7.

$$R_{fi,d,t} \geq E_{fi,d} \text{ at } t = t_{req} \tag{2}$$

This verification is proposed as the standard method in Eurocode 3. It can be shown that, in the case of a fire with no decreasing phase, the fact that Equation (2) is satisfied guarantees that Equation (1) is also satisfied, see Figure 6. On the other hand, in the case of a fire with a cooling down phase, it can happen at some stage that Equation (1) is satisfied whereas Equation (2) is not satisfied, as show in Figure 7.

2.2.3 Safety verification in temperature domaine

At the required fire resistance time t_{req}, it has to be verified that the temperature of the structure $\theta_{structure}$ is still lower than the critical temperature θ_{cr}, the temperature that leads to failure. This is expressed by equation (3) and corresponds to the verification on Figure 6 and Figure 7.

$$\vartheta \leq \vartheta_{cr} \text{ at } t = t_{req} \tag{3}$$

This verification is a particular case of the verification in the load domain, only possible when the stability of the structure is depending on a single temperature, which is the case in steel elements under uniform temperature distribution. It can also happen for natural fires that Equation (3) is satisfied whereas Equation (1) is not.

The verification in the load domain has indeed several advantages wich is: 1- It is easy to use; because the verification is at a given time; the steel temperature and hence the material properties are known and can be used for the evaluation of the load bearing capacity. 2- It is applicable for any type of effect of actions whereas, as will be explained in Section verification in the temperature domain is possible only in a limited number of cases. 3- It produces a safety factor that is similar to the one that engineers and designers have been using for years at room temperature, namely the ratio between the applied load and the failure load. On the other hand, verification in the temperature domain yields a safety factor in degrees centigrade that does not provide much in term of practical consequences. A verification in the time domain may even be more confusing because, with the tendency of standard fire curves to level off at nearly constant temperatures after a certain period of time, they can yield the false impression of a very high level of safety because the calculated time of failure is significantly longer than the required fire resistance time, simply because the temperature of the structure changes very slowly, whereas a small variation in the applied load or in the heating regime would decrease the fire resistance time very dramatically close to the required resistance time, [11].

2.3 Steel temperature development of unprotected internal steelwork

If the temperature distribution in the cross section is supposed to be uniform, the temperature increase during a time increment is given by this Equation (4).

$$\Delta\theta_{a,t} = k_{sh} \frac{\frac{A_m}{V}}{C_a \rho_a} \dot{h}_{net} \, \Delta t \tag{4}$$

For I-sections under nominal fire actions, the correction factor for the shadow effect may be determined from:

$$\text{ksh} = 0.9\ [\text{Am/V}]\text{b}/[\text{Am/V}] \tag{5}$$

Where: [Am/V]b is box value of the section factor

In all other cases, the value of ksh should be taken as: ksh = [Am/V]b/[Am/V].

The previous equation 4 is better understood if transformed into the form of Equation (6) which shows that it is just the expression of the conservation of energy between the quantity that penetrates in the section and the quantity used to modify the temperature and hence the enthalpy of the section.

$$\dot{h} \times \mathrm{k_{sh}} \times A_m \times \Delta t = \Delta\theta_{s;t} \times ca \times \rho a \times V \tag{6}$$

In this equation, the ratio between the surface area of the member and the volume of the member, Am/V, is the parameter characterising the cross section of the member that governs its heating.

The term of "section factor'' is not meaningful because it contains no information about the physical characteristic that this factor represents. This parameter is sometimes referred to as "the massivity factor'' which indicates at least what this factor is about, but the problem nevertheless remains that this quantity is the highest for the most slender and less massive sections.

2.4 Internal steelwork insulated by fire protection material

If the temperature distribution in the cross section is supposed to be uniform, the temperature increase during a time increment is given by Equation (7).

$$\Delta\theta_{a,t} = \frac{\frac{\lambda_p A_p}{V}}{d_p c_a \rho_a} \frac{(\theta_{g,t} - \theta_{a,t})}{(1 + \frac{\phi}{3})} \Delta t - (e^{\phi/10} - 1)\Delta\theta_{g,t} \tag{7}$$

$$with\ \phi = \frac{c_a \rho_p}{c_a \rho_a} d_p A_p / V$$

The above equation is derived from the formulation where the governing partial differential equation of the heat transfer inside the insulation layer was solved. Some simplifications of the solution of this 1D equation lead to the exponential correction factor. Strictly speaking, the approximation of the exact solution is valid for small values of the factor ϕ .this factor should normally not be higher than 1.5 but this limitation has not been specified in the Eurocode.

2.5 Nominal fire curves- Models Eurocode

Nominal fire curves are the simplest and most used as a means of representation of a fire. Although they do not represent real fires, they were established from experience on

real fires and are the most frequently used. They are represented by conventional models of curves given by the Eurocode 1 part 1-2 and adopted for classification or verification of the fire resistance. The best known are the standardized fire curve ISO 834, presented in **Erro! A origem da referência não foi encontrada.**, the external fire curve, the hydrocarbon curve,[12].

2.5.1 Standard fire curve ISO 834

For the modeling of a fire in a building, the ISO 834 curve is a conventional reference. The temperature evolution over time showed in Figure 8 and given by the following equation:

$$= 20 + 345\log10(8 \quad + 1) \tag{8}$$

Where θ represents the gas temperature in the compartment, in [°C], and t represents the time, in minutes.

Conventional fire curve must be applied to the entire enclosure which size needing and not dependent fire development conditions, or possibility of previous fires its generalization. Finally it is important to note that his appearance and ascending in heating only.

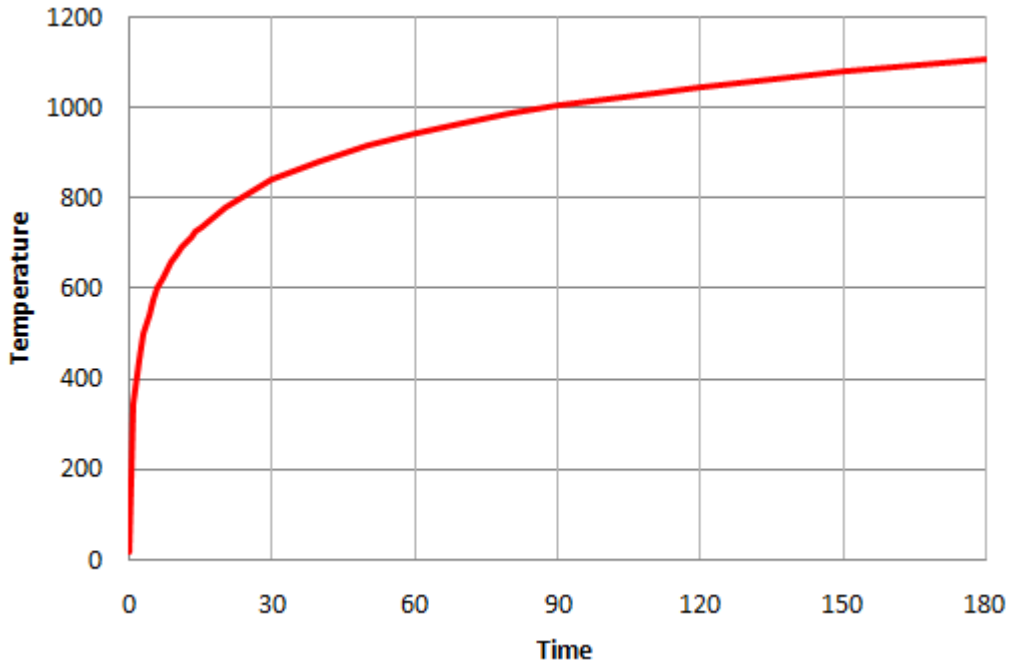

Figure 8: Standard fire curve ISO834.

Figure 8 showed a nominal fire curve this curve are used to test the fire resistance of materials this standard is the least'intensive' of the fire curves.

2.5.2 Curve of hydrocarbons

Developed in the 70s by the oil company Mobil, it has an up speed temperature with a temperature of 900 [°C] within the first five minutes. This research was initiated to develop a test procedure for assess the protection materials against fire for offshore drilling platforms and oil facilities.

The curve of temperature is given by:

$$\theta = 20 + 1080 \left(1 - 0.325^{-0.167} - 0.675^{-2.5}\right) \quad (9)$$

2.5.3 External fire curve

If the structure whose fire resistance is desired to know is considered a field structure or a compartment lying below or next to outer wall, one may use an external fire curve, given according to the equation (10).

$$\theta = 20 + 660 \left(1 - 0.687^{-0.32} - 0.313^{-3.8}\right). \quad (10)$$

2.6 Steel temperature evolution from simplified method

To determine the temperature evolution of differente beams a set of two scripts were developed in Matlab. One to study the behaviour of beams with fire protection material, gypsum, and the second for solid and cellular beams without fire protection. This calculations were done taking into consideration the hole diameter calculated from the beam hight and equal to D=0.714xh, and a distance between center of holes given by S=1.5D. These routines are presented in the Anexes.

A parametric analysis was done, considering differente sections exposed to 3 sides and 4 sides, for cellular and solid beam without protection. Table 1 compare the section factores of both solid and cellular beams exposed to 3 and 4 sides.

Section factor for unprotected solid and cellular beams are determined;

$$\left[\frac{A_m}{V}\right]_b = \left[\frac{\text{box surface area per unit length}}{\text{volume of the member per unit length}}\right]$$

For section factor of unprotected solid beams exposed to fire in 4 sides was calculated:

$$\left[\frac{A_m}{V}\right] = \left[\frac{(4*b + 2*(h - tw - 4*r) + 2*\pi*r)}{A}\right]$$

For section factor of unprotected solid beams exposed to fire in 3 sides was calculated:

$$\left[\frac{A_m}{V}\right] = \left[\frac{(3*b + 2*(h - tw - 4*r) + 2*\pi*r)}{A}\right]$$

For section factor of unprotected cellular beams exposed to fire in 4 sides was calculated:

$$\left[\frac{A_m}{V}\right] = \left[\frac{(4\times b + 2\times(h - tw - 4\times r) + 2\times\pi\times r) - nh\times Ah\times 2 + nh\times Hp\times tw}{A\times L - nh\times Ah\times tw}\right]$$

Where: nh= ((L+0.714*h)/(1.5*0.714*h))-1

Section factor for the web

$$\left[\frac{A_m}{V}\right] = \left[\frac{((2\times h) - (4\times tf))}{(h - 2\times tf)\times tw}\right]$$

Section factor for the flange

$$\left[\frac{A_m}{V}\right] = \left[\frac{(2\times b + 2\times tf) - tw}{b\times tf}\right]$$

The section factor for the cellular beam is smaller than the one from solid beams for all sections and in the both types of fire exposure.

Table 1: Section factor for unprotected cellular and solid beams.

CASE	SEC	S-SF[m^{-1}]		h	D=	S=	C-SF[m^{-1}]	
		4side	3side	[mm]	0.714*h	1.5*D	4sides	3sides
1	IPE100	388.13	334.74	100	71.4	107.1	380.82	318.48
2	IPE160	309.72	268.92	160	114.24	171.36	299.74	251.58
3	IPE200	269.54	234.45	200	142.8	214.2	260.96	220.82
4	IPE300	215.62	187.74	300	214.2	321.3	207.73	175.21
5	HEB100	218.23	179.64	100	71.4	107.1	212.87	170.92
6	HEB160	169.10	139.64	160	114.24	171.36	164.53	132.13
7	HEB200	147.38	121.77	200	142.8	214.2	143.65	116.006
8	HEB300	116.13	96.01	300	214.2	321.3	112.06	90.20

The temperature evolution in function of time for diferente unprotected sections, solid and cellular beams made from IPE100, is shown in Figure 9. A similar result is presented from Figure 10 to Figure 16, for the other sections of Table 1.

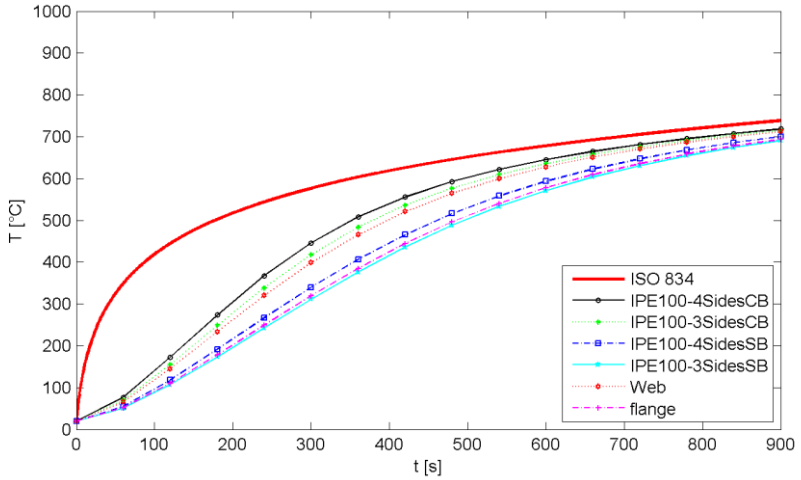

Figure 9: Temperature evolution for unprotected cellular and solid beam IPE100.

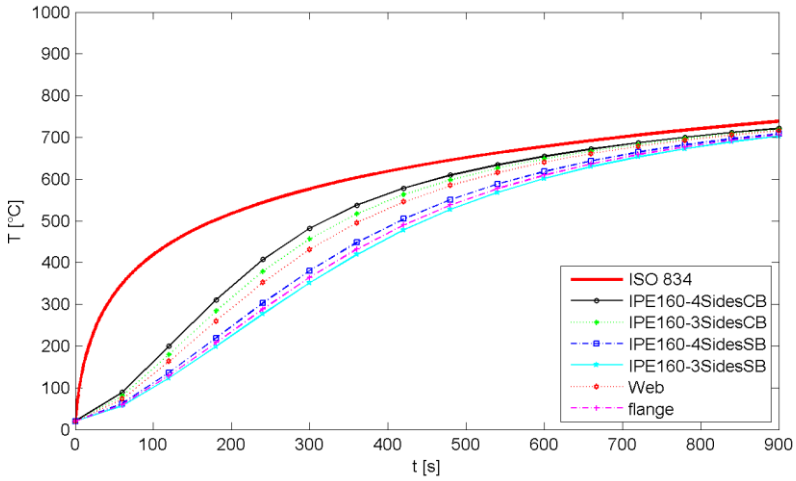

Figure 10: Temperature evolution for unprotected cellular and solid beam IPE160.

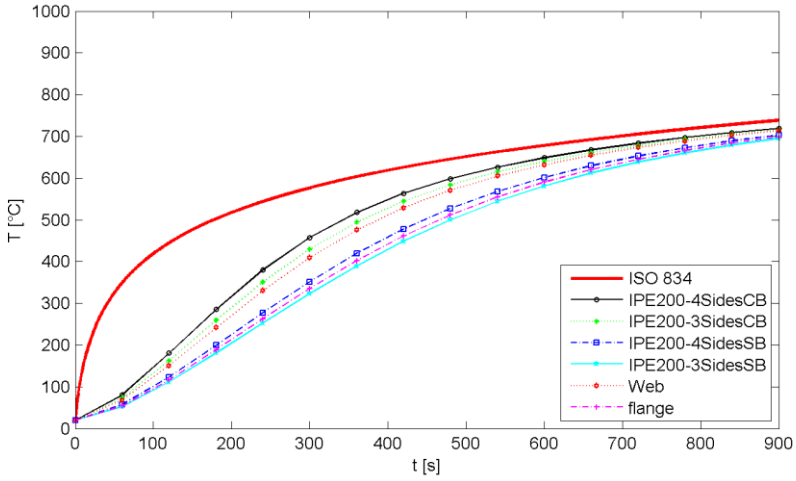

Figure 11: Temperature evolution for unprotected cellular and solid beam IPE200.

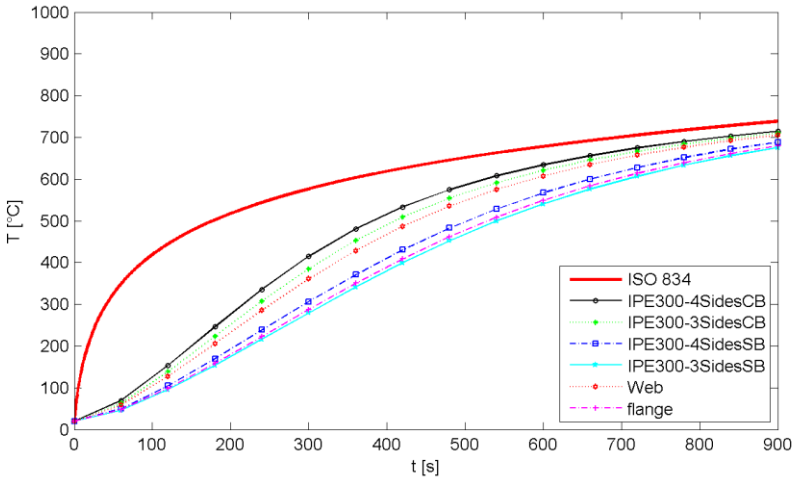

Figure 12: Temperature evolution for unprotected cellular and solid beam IPE300.

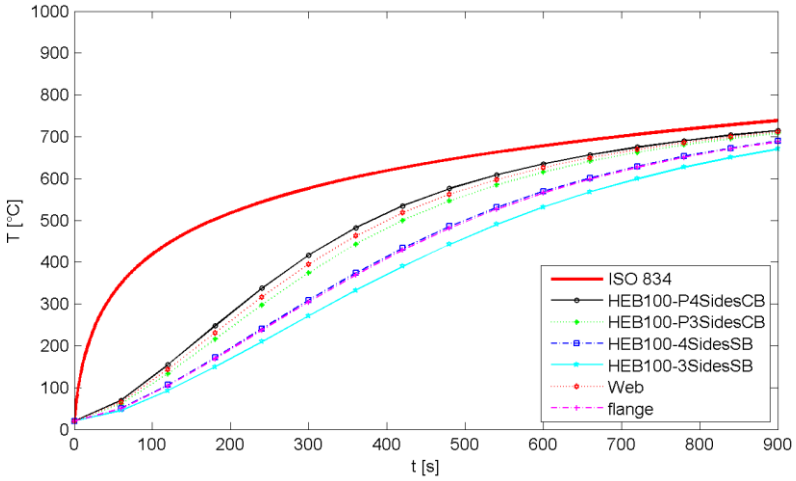

Figure 13: Temperature evolution for unprotected cellular and solid beam HEB100.

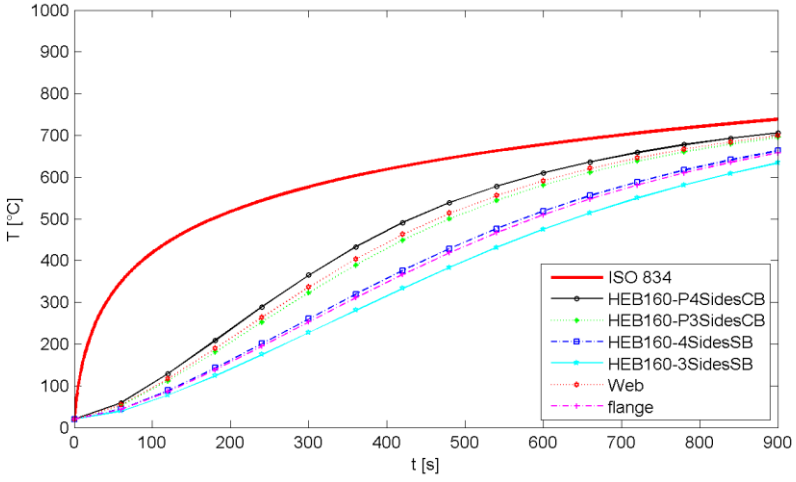

Figure 14: Temperature evolution for unprotected cellular and solid beam HEB160.

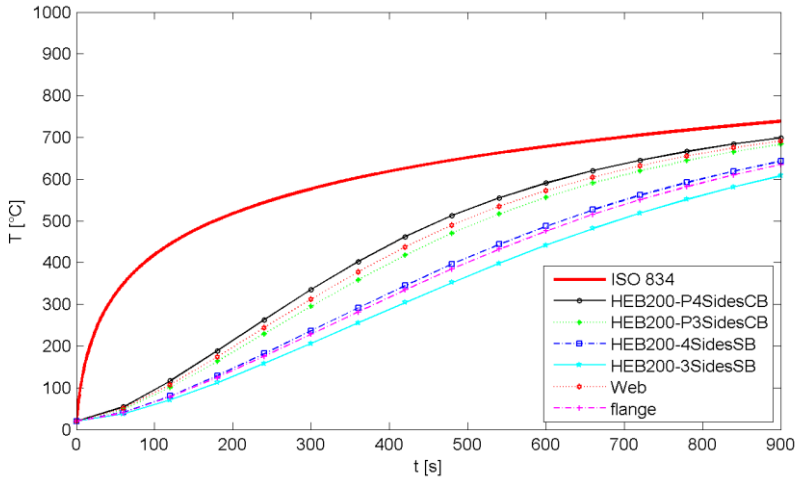

Figure 15: Temperature evolution for unprotected cellular and solid beam HEB200.

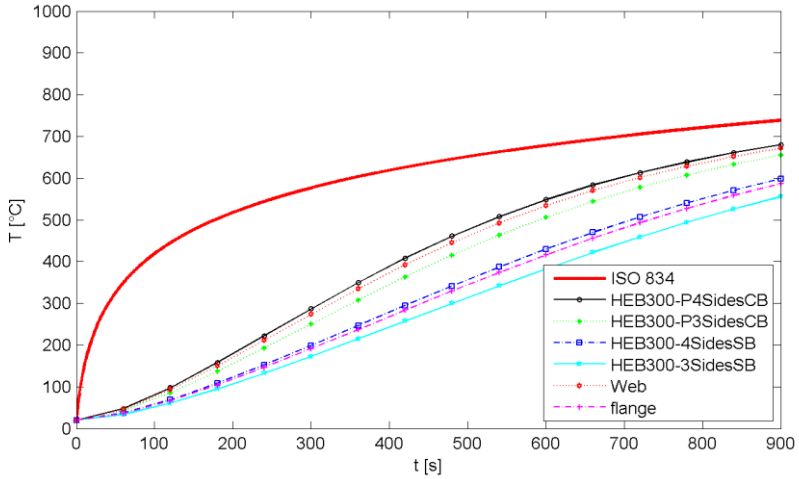

Figure 16: Temperature evolution for unprotected cellular and solid beam HEB300.

From the simplified method the section factor Am/V of unprotected solid beams in 3 sides are reduced compared to that heated on 4 sides in all section. Also the same case for unprotected cellular beams.

To study the behaviour of solid and cellular beams with fire protection, a similar study was done considering both types of sections protected with Gypsum boards. This material was chosen due to its well known thermal properties in function of temperature. The thermal properties considered for this calculation are:

dp = 23 mm Thickness of gypsum

rhop = 800 kg/m^3 Density of gypsum

Cp = 1700 J/kg°K Specific Heatof gypsum

kp = 0.2 W/m°K Thermal Conductivity of gypsum

mc = 20% Moisture content

The sections studied are presented in Table 2 for fire exposures from 3 and 4 sides.

Table 2: Section factors for protected cellular and solid beams.

CASE	SEC	S-SF [m^{-1}]		h	D=	S=	C-SF [m^{-1}]	
		4sides	3sides	[mm]	0.714*h	1.5*D	4sides	3sides
1	IPE100	388.13	334.74	100	71.4	107.1	326.20	272.80
2	IPE160	309.72	268.92	160	114.24	171.36	253.88	213.09
3	IPE200	269.54	234.45	200	142.8	214.2	228.11	193.02
4	IPE300	215.62	187.74	300	214.2	321.3	178.09	150.21
5	HEB100	218.23	179.64	100	71.4	107.1	195.16	156.70
6	HEB160	169.10	139.64	160	114.24	171.36	149.62	120.16
7	HEB200	147.38	121.77	200	142.8	214.2	133.05	107.44
8	HEB300	116.13	96.01	300	214.2	321.3	103.12	83.00

The temperature evolution in function of time for diferente protected sections, solid and cellular beams made from IPE100, is shown in Figure 17. A similar result is presented from Figure 18 to Figure 20, for the other sections of Table 2.

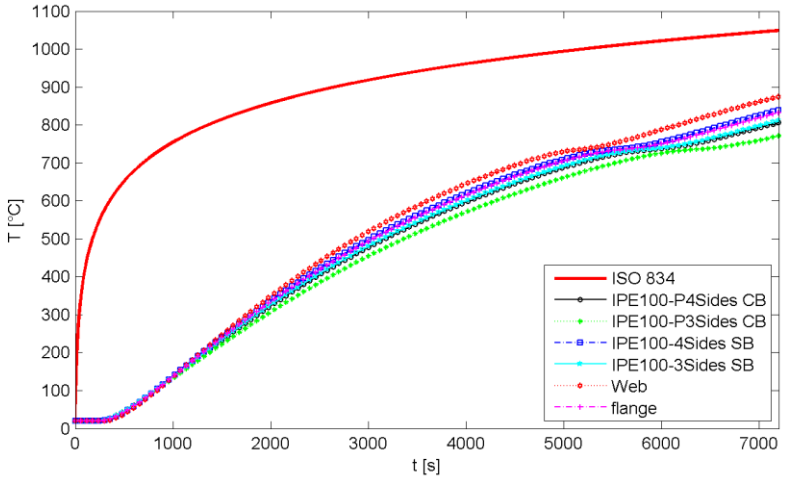

Figure 17: Temperature evolution for protected cellular and solid beam IPE100.

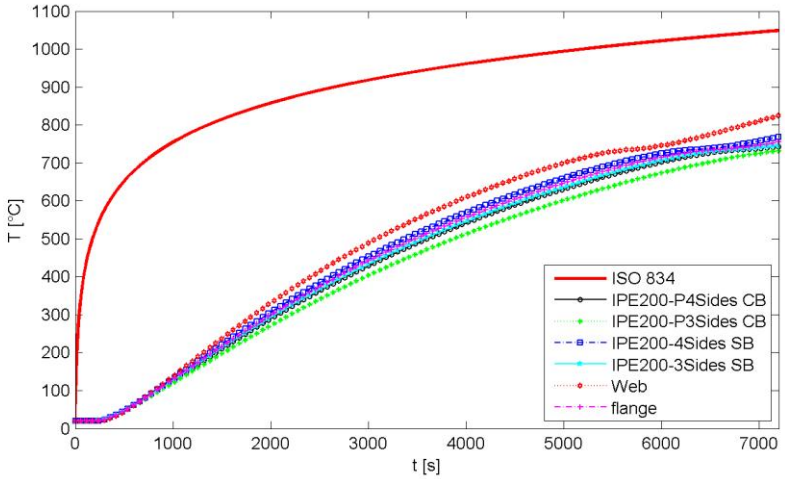

Figure 18: Temperature evolution for protected cellular and solid beam IPE200.

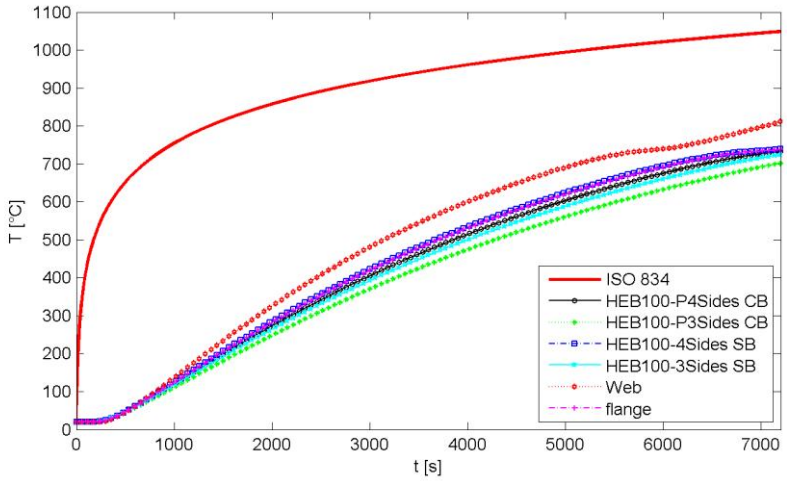

Figure 19: Temperature evolution for protected cellular and solid beam HEB100.

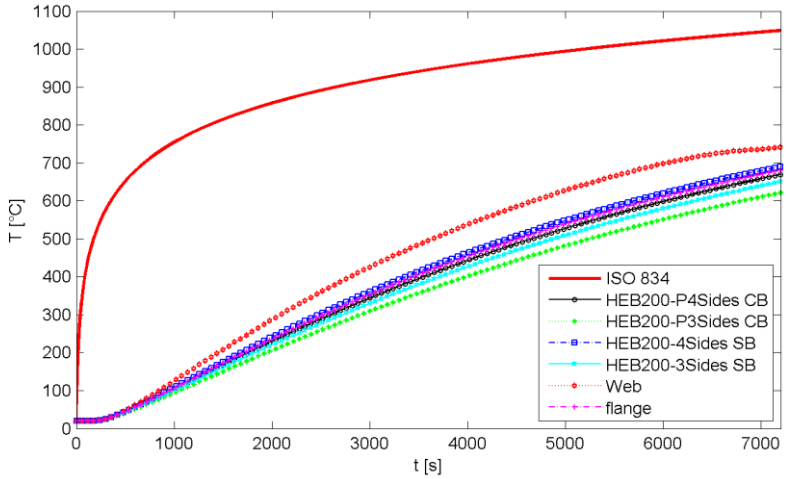

Figure 20: Temperature evolution for protected cellular and solid beam HEB200.

The simulation of solid and cellular beams protected with gypsum showed that the section factor for 3 sides and 4 sides are higher than cellular beams in the both sides for all section. The section factor for sections insulated by a hollow encasement are based on the dimensions of the section, h and b, even if the encasement does not touch the section and, in that case, the surface that radiates energy to the steel section is the inside surface of the encasement.

2.6.1 Influence of section factor

The degree of fire protection depends on the A/V section factor for the steel section. The A/V factor is a function of the area of the steel exposed to the fire and the volume of the steel section. The higher the A/V, the faster the steel section heats up, and so the greater the thickness of fire protection material required. The section factor and limiting temperature are used to determine the thickness of protection required.

The section factor is a way of describing the heating rate of a member, which is a key factor in determining fire resistance for that section. The shape of the member governs the time taken for it to reach its failure or limiting temperature and varies according to the relative dimensions of the section. A heavy, massive section will heat up more slowly than a light, slender section. This effect is quantified in the section factor.

The section factor is also dependent on whether a boxed out fire protection system or a coating-based section profile system is adopted and on whether or not the section is carrying a floor slab. Where a section is partially protected, for example when a column is built into a perimeter wall, the section factor should be calculated as standard tables do not represent this arrangement.

The results showed that the section factor is a very important concept when using protection for the beams. Also the unprotected beams take longer to heat to a set critical temperature than a relatively slender section of high section factor.

Section factor it is a measure of how quickly the steel section will heat in a fire, and therefore how much fire protection is required.

2.6.2 Influence of shadow effect

The effect of the shadow factor, or correction factor, is to change the section factor As/V to that of the box enclosing the steel section. Nominally, the box represents the effective boundary of the steel section to the radiant heat flux and is introduced to allow for the assumption that radiant heat transfer to the concave surfaces is blocked by the shadow of the cross section. However, examination of the background documents [13, 14] indicates that the principal reason for introducing this so-called shadow effect is due to the different values of resultant emissivity recommended in the two different versions of Eurocode 3 Part 1.2, being 0.5 in ENV 1993-1-2 (CEN 1993–1995) and 0.7 in EN 1993-1-2 (CEN 1993– 2005b). Therefore, the real purpose of the shadow effect is to compensate

for the overestimation of steel temperature in EN 1993-1-2 caused by using a higher value of resultant emissivity.

To study the influence of this factor the sections studied in the previous sections were analysed considering unit shadow factor and the value calculated as prescribed by the Eurocode 3 part 1.2, [15].

The Table 3 and Figure 20, Figure 22 show the results from the temperature evolution of an IPE160 section considering diferent values of the shadow effect, $K_{sh}\neq1$ and $K_{sh}=1$, for a fire exposure from 4 sides. For a cellular beam made from an IPE300 reach a temperature of 500 [ºC] it must be exposed for 611,25 and [s] 507,8 [s], considering respectively $K_{sh}\neq1$ and $K_{sh}=1$, when exposed in 4 sides. When it is exposed to fire from 3 sides it reaches 500 [ºC] afeter 677.91 [s] and 553.63 [s], respectively.

Table 3: Exposure time to reach a reference temperature of 500 [°C] and 600 [°C] for a shadow effect Ksh≠1 and Ksh =1

Section	**Temp.**	$k_{sh}\neq1$		$k_{sh}=1$				**web**	**Flange**
		SB and CB		**SB**		**CB**			
		4 side	**3 side**	**4side**	**3 side**	**4side**	**3 side**		
IPE 100	500	444.24	492.65	370.34	398.54	373.8	408.69	332.19	377.05
	600	595.4	650.55	514.13	544.57	517.82	555.72	474.76	521.3
IPE 160	500	500.06	553.34	414.54	445.91	420.18	458.63	364.95	431.54
	600	659.08	720.86	562.19	597.28	568.45	611.6	508.43	581.33
IPE 200	500	537.95	595.14	445.38	479.4	452.99	495.03	385.84	464.61
	600	702.94	769.76	596.69	635.36	605.29	653.3	530.75	618.49
IPE 300	500	611.25	677.91	501.42	540.67	507.8	553.63	435.28	528.33
	600	788.67	867.31	660.66	706.10	668.00	721.2	585.32	691.77
HEB 100	500	640.87	756.16	498.19	553.74	504.91	569.42	399.38	503.47
	600	823.55	960.1	656.93	721.32	664.68	739.63	545.49	663.02
HEB 160	500	746.86	884.53	572.59	637.79	579.99	654.33	463.34	585.65
	600	949.06	1113	743.59	819.93	751.99	839.45	617.04	758.63
HEB 200	500	810.72	961.89	618.62	689.60	627.64	709.15	493.35	636
	600	1025	1205.4	797.34	881.14	807.96	904.30	651.37	817.82
HEB 300	500	935.44	1113	708.68	791.58	718.15	810.41	550.28	731.29
	600	1173.8	1386.3	903.75	1002.2	914.97	1024.6	717.3	930.56

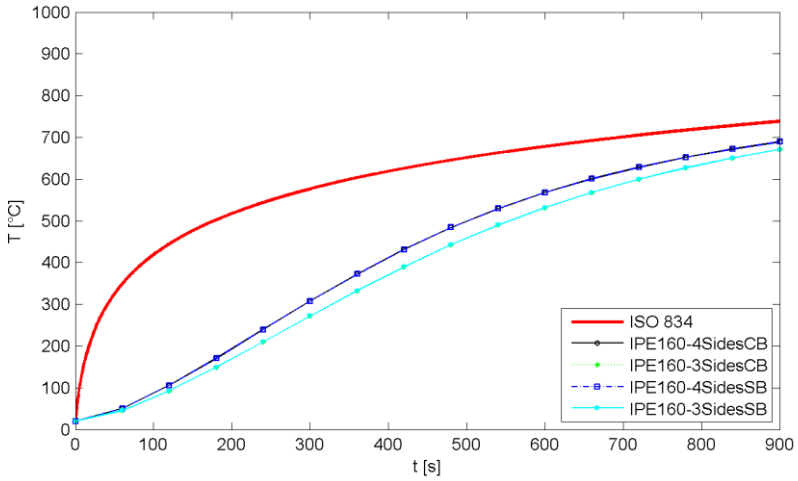

Figure 21: Influence of shadow factor for IPE160 with shadow effect different than1.

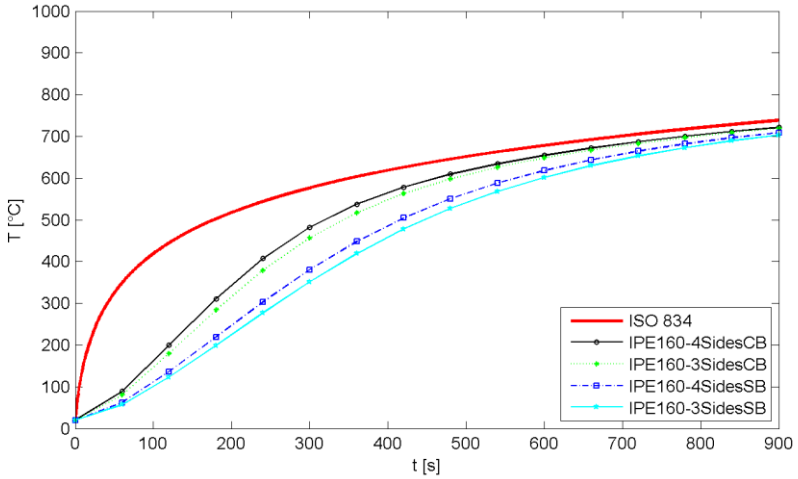

Figure 22: Influence of shadow factor for IPE160 with shadow effect equal to 1.

Table 4: Steel temperature values for a fire exposure time equal to 30 [min] and 60 [min] for a shadow effect Ksh≠1 and Ksh =1.

Section	Time (min)	k_{sh}≠1		k_{sh} =1				Web	Flange
		SB ans CB		SB		CB			
		4side	3 side	4side	3 side	4side	3 side		
IPE 100	30	703.53	691.43	715.78	711.83	715.34	710.21	720.16	714.91
	60	833.75	830.85	836.63	835.66	836.52	835.28	837.79	836.41
IPE 160	30	689.25	670.91	709.22	703.17	708.23	700.32	716.46	706.11
	60	830.28	824.75	835.06	833.67	834.83	833.01	836.8	834.34
IPE 200	30	676.67	563.59	703.29	695.11	701.61	690.74	713.71	698.89
	60	826.64	818.14	833.7	831.77	833.31	830.67	836.11	832.68
IPE 300	30	646.35	614.04	688.84	675.68	686.87	670.8	705.37	680.08
	60	814.97	798.05	830.17	826.32	829.64	824.71	834.17	827.69
HEB 100	30	632.38	573.77	689.81	670.76	687.77	664.53	711.7	688.21
	60	808.17	772.99	830.42	824.7	829.88	822.47	835.63	830
HEB 160	30	578.62	507.68	663.13	633.86	660.13	625.8	699.2	657.72
	60	776.04	740.8	821.95	808.93	820.8	804.69	832.75	819.84
HEB 200	30	545.33	470.28	642.94	608.12	638.71	598.14	691.23	634.72
	60	756.31	733.62	813.39	794.53	811.36	788.39	830.79	809.37
HEB 300	30	482.78	405.52	598.38	555.29	593.51	545.5	672.08	586.72
	60	735.51	706.53	788.54	761.81	785.48	756.39	825.14	781.18

The Table 4 show the results from the temperature evolution of many section considering diferent values of the shadow effect, K_{sh}≠1 and K_{sh} =1, for a fire exposure from 4 sides and 3 sides. For the Figure 23, Figure 24 and Figure 25, Figure 26 presented the results from the temperature evolution of an secion IPE100 and IPE 300 for cellular and solid beam with Ksh =1 and k_{sh}≠1 respectivly . For the case of Ksh =1 we have different temperature evolution for 30 min and 60 min for the both sides and when k_{sh}≠1 the results the same for cellular and solid beams and in the both side.

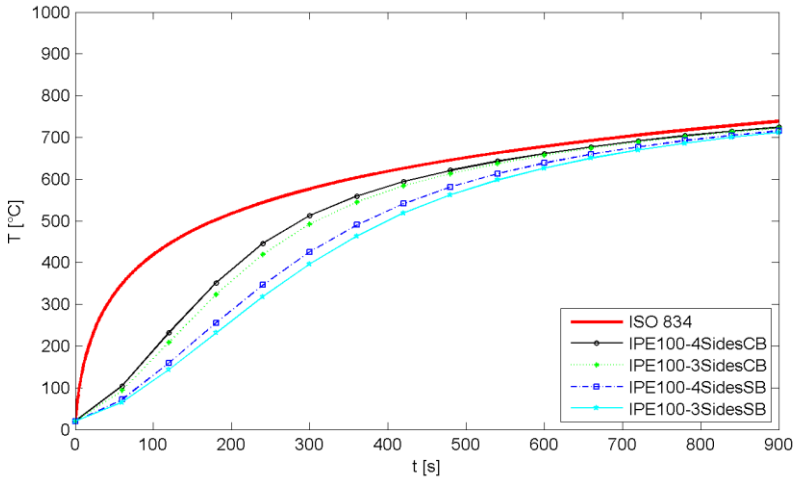

Figure 23: Temperature evolution for cellular and solid beam for IPE100 with Ksh=1

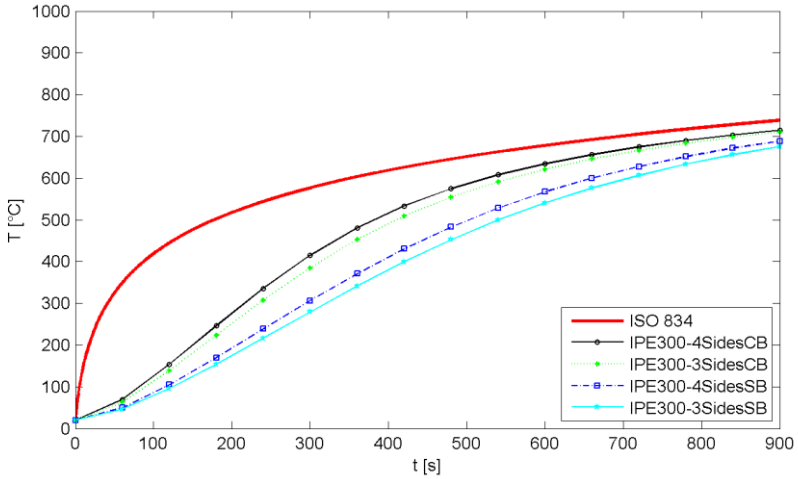

Figure 24: Temperature evolution for cellular and solid beam for IPE300 with Ksh=1

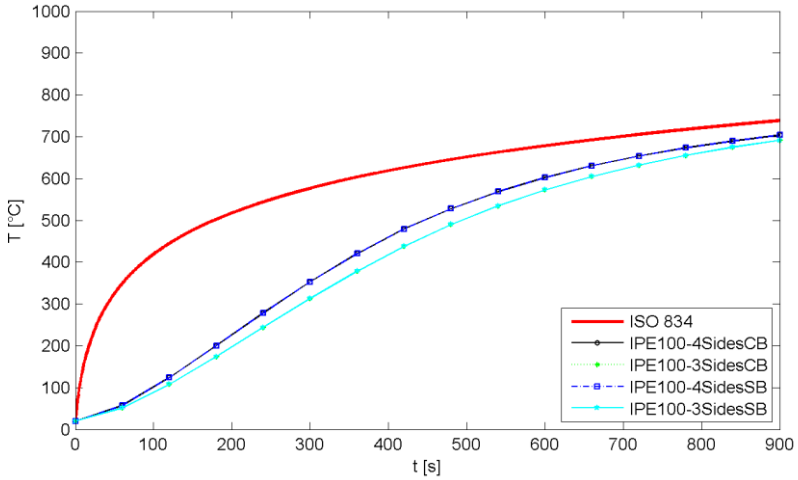

Figure 25: Temperature evolution for cellular and solid beam for IPE100 with Ksh≠1.

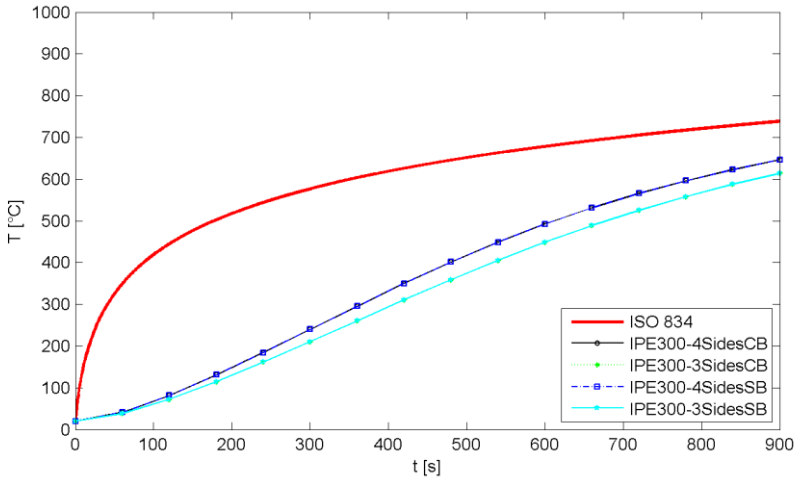

Figure 26: Temperature evolution for cellular and solid beam for IPE300 with Ksh≠1

2.7 Fire resistance tests of cellular beams accordingly to EN13381-9

The fire resistance standard EN13381-9 adopts the principle of establishing ratios of temperatures between and around openings in the web of a beam with the temperatures of a solid portion of that beam. The aim is that this data can be utilized within a structural model to derive the value and location of the associated limiting temperature of the beam at the fire limit state. This can then be used in conjunction with data for the fire protection material,[16].

Also applies to fire protection materials that have already been tested and assessed in accordance with EN 13381-4 or EN13381-8. This Standard cannot be used in isolation. The use of this Standard requires the multi-temperature analysis (MTA) derived from EN 13381-4 or EN 13381-8 as the basis for determining thickness for beams with web openings, [17].

The assessment procedure is used to establish: a) On the basis of the temperature data derived from testing unloaded steel/sections, the thermal response of the fire protection system on cellular beams, (the thermal performance). b) The temperature ratio between the web post and the web reference temperature, which will vary depending on the web post width. c). The temperature ratio between points around the web openings and the web reference area. d) The elemental multi temperature analysis from either EN 13381-4 or EN 13381-8 shall be reassessed and reported against elemental A/V for each fire resistance period. e) A structural model shall be used to derive limiting temperatures for cellular beams.

2.7.1 Elemental multi-temperature analysis

The fire protection thickness applied to any cellular beam must be sufficient to keep the beam below its limiting temperature. The thickness required for each fire resistance period is determined from the EMTA generated by the assessment from EN 13381-4 or EN 13381-8.

The structural model will indicate whether failure is governed by the web or the bottom flange limiting temperatures so that the most appropriate elemental analysis can be used to determine the fire protection thickness.

The fire protection thickness applied to any cellular beam must be sufficient to keep the beam below the temperatures derived from a structural analysis at elevated temperatures.

The web or bottom flange temperature for a given thickness of fire protection shall be obtained by carrying out an assessment to EN 13381-4 or EN 13381-8 for the web or bottom flange temperatures only. The web or bottom flange temperatures are analyzed in the same way that average beam temperatures are analyzed with the exception that the stick ability correction factors used are those for already used for the average beam temperature Where the assessment is based on short column testing only, the assessment shall be carried out using the mean of both flanges, [17].

Conservatively, the web and bottom flange temperatures may be assumed to be equal and the section factors of the individual web and flange.

The fire protection thickness shall be that derived from an assessment in accordance with 13381-4 or EN 13381-8 , [17].

2.7.2 Procedure and steps of tests according to European standart EN13381-9

The test method for determining the contribution to the fire resistance of structural members made from fire protection materials to the fire resistance to steel beams with web opening follow the standard EN13381-9. The thermocouple consistency and the data points for temperature is specified in EN 1363-1, [18].

During the test furnace temperature must be measured and recorded in the region of the test specimens using the plate thermometers defined in EN 1363-1 and the furnace pressure in accordance with EN 1363-1. Also the steel temperature must be measured and recorded using the thermocouples attached to the steelwork as specified at intervals not exceeding 1 minute.

Some monitoring must be done regarding the general behaviour of each of the specimens throughout the test and record the occurrence of cracking, fissuring, delamination or detachment of the fire protection material and similar phenomena as described in EN 1363-1,[18].

The test must continue until the required fire performance period is reached. If the mean bottom flange temperature recorded on all the steel sections has not reached 575 [ºC] then the test shall be continued until this occurs and this must be within 15% of the required fire resistance period. If the maximum temperature in the scope of the multi-temperature analysis generated from EN 13381-4 or EN 13381-8 is less than 575 [ºC] then this shall be used instead of 575 [ºC] for termination of the test,

2.8 Temperature verification for the web and flange:

The web post is divided into 3 zones: 2 edge zones of width E and a central zone of width D. The web post average temperature is always given by:[(temp at A) x E + (temp at C) x E + (temp at B) x D] / web post width P.

For different web post widths, the dimension ‘a’ must be determined. The influence of the higher edge temperatures is not considered to be at more than twice the thermocouple position from the edge of the opening. Therefore ‘a’ is limited to 25 mm. This limit applies for post widths greater or equal to 150 mm (at 150mm, ‘a’ equals 25 mm).

Posts >= 150 mm

Thus for a post width greater or equal to 150 mm the web post average temperature is given by: [(temp at A) x 50 + (temp at C) x 50 + (temp at B) x (P – 100)] / web post width, P.

Posts <150 mm

For post widths less than 150 mm dimension E is given by: E = 25 + a, with D given by 2a. from this results: P = 2 (25 + a) +2a and a = (P – 50)/4.

This gives the result that for a post of 50mm, ‘a’ is zero and this method of averaging therefore cannot be used for narrower posts.

The general formula for the average web post temperature for posts between 150 and 50mm is given by: [(temp at A) x (25 + a) + (temp at C) x (25 + a) + (temp at B) x 2a] / P

For a 100mm web post this equqtion is more conservative:

(temp at A) x 37.5 + (temp at C) x 37.5) + (temp at B) x 25] / P.

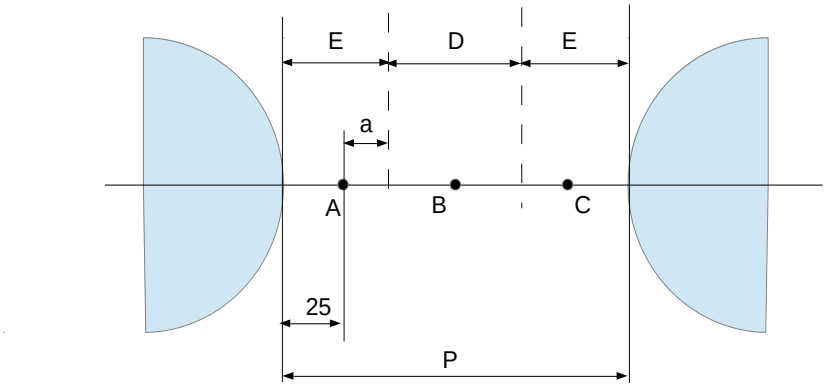

Figure 27: Position of the thermoucouple according to EN13381-9.

Chapter 3: Fire resistance tests of solid and cellular beams

3.1 Introduction

The intumescent fire protection thickness required to provide a given fire resistance to a cellular beam depends on its web thickness, the hole shape and dimensions, the width of the web post, the degree of the beam asymmetry and the structural utilisation factor, as well as the protection efficiency of the intumescent coating. A common method to achieve the required fire resistance of cellular beams is to apply an intumescent coatingto the steel. The results of Bailey work ,[6] show that the difference between the web post and bottom flange temperatures depends on type and thickness of the intumescent fire protection.

3.1 Intumescent Coatings

Intumescent coatings have been used to protect the steelwork in buildings and other structures from fire for approximately 40 years. These coatings work by swelling up in the event of fire and physically creating a barrier between the steel and the fire for up three hours. Steel loses part of its structural strength at about 500 [ºC] and these coatings can delay the time it takes to reach this temperature also intumescent coatings provide fire protection by undergoing an endothermic decomposition reaction process at the elevated temperatures that causes the material to swell and foam into a highly porous, thick and thermally stable char layer. The high void content and thickness of the coating allow it to act as an insulation barrier to the underlying substrate against flame and heat, [19].

An intumescent coating can be applied by painting or spraying a liquid compound onto structural elements. The compounds cure in the air over several hours into a solid intumescent film. The maximum coating thickness that can be achieved with this method is under about 5 [mm]. Thicker coatings are applied by bonding of fibrous intumescent mat directly onto the substrate using high-temperature adhesive paste. The fire protection provided by intumescent coatings occurs by three reaction processes witch is: 1-The coating material decomposes, 2-Inert gases evolved from the decomposition reaction are produced at a high enough rate to drive back hot convective air currents, and most importantly, 3-The coating expands into a highly porous char layer with a high resistance to heat conduction from the flame into the underlying composite ,[20]

Intumescent coatings contain ‘active’ ingredients bound together by a binder. Generally, three ‘active’ ingredients are used: an acid source (normally ammonium polyphosphate (APP)) or a mineral acid), a carbon source (such as pentaerythritol (PER) or polyols) and a blowing agent (normally melamine (MEL)), [19].

The use of intumescent coatings plays an important role in the fire protection of structural elements witch is: When submitted to elevated temperatures an intumescent coating undergoes thermochemical reactions that promote a higher thermal protection. Intumescent coatings provide fire protection by undergoing an endothermic decomposition reaction process at the elevated temperatures that causes the material to swell and foam into a highly porous, thick and thermally stable char layer.

A typical example of an intumescent coating is shown in figure 28. It has expanded to many times the original thickness. A good intumescent coating expands 50 to 200 times, and forms a fine-scale multicellular network with a cell size of 20 to 50 μm and wall thickness of 6-8 μm, [19].

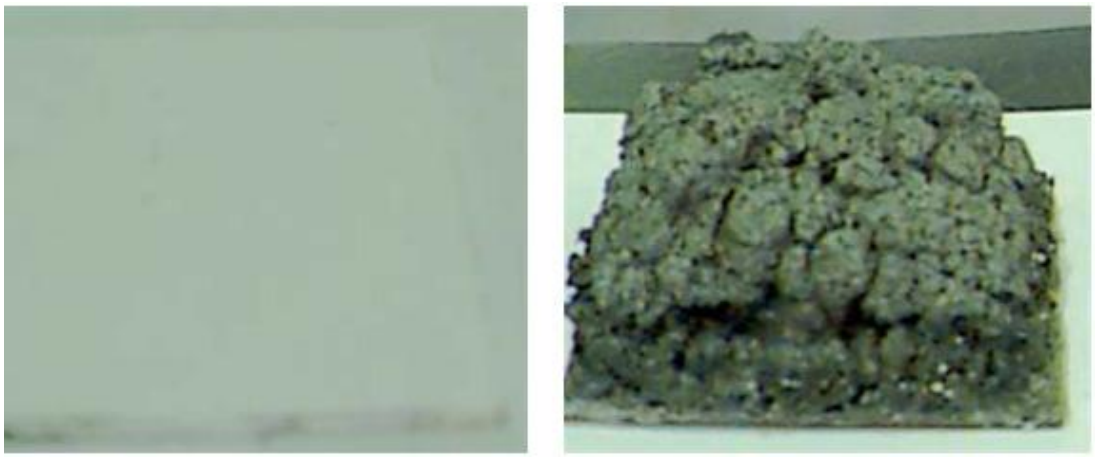

Figure 28:Intumescent coating (a) before fire test and (b) after fire testing, [19].

The temperature of the web-post in a cellular beam increases at a faster rate compared to its equivalent (similar web size) solid beam. If the temperature of the web-post increases faster than expected than the cellular beam failure may occur by local buckling instability of the web-post between the openings or the Vierendeel bends at the opening. Intumescent coatings consist of a mix of compounds that each has a role in the Intumescence process. The four main types of compounds are a carbon-rich (carbonific) compound, inorganic acid or acid salt, organic amine or amide, and a blowing agent (spumific). For intumescence to occur these compounds must undergo a series of

decomposition reactions and physical processes almost simultaneously, but within a proper sequence. The order of these processes. If the time between the processes is too long or they do not occur in the correct order, then the coating will fail to intumesce, [19].

3.2 Experimental setup and elements instrumentation

The set of experimental tests performed at the Polytechnic Institute of Bragança to evaluate the behaviour of solid and cellular beams with and without fire protection is the presented in

Table 5. The table shows the set of performed experimental tests considering solid beams with and without intumescent protection and also cellular beams with and without intumescent fire protection. The aim was to consider for all tested beams the same nominal intumescent DFT, equal to 1000 [μm], but as can be seen in the table the coating of the test P4 has resulted in a little higher DFT. A water based intumescent coating supplied by International Coatings was used. Also were studied different combinations of the hole diameters and web post widths.

Table 5: Geometries and properties of the tested beams.

Ref.	**Beam type**	**DFT [μm]**	**D [mm]**	**W [mm]**
P1	Solid			
P2	Solid	-	-	-
P3	Solid	1047,3	-	-
P4	Solid	1187,5	-	-
P5	Cellular	-	120	60
P6	Cellular	-	120	60
P7	Cellular	860,4	120	60
P8	Cellular	1311,0	120	60
P9	Cellular	-	120	75
P10	Cellular	960,4	120	75
P11	Cellular	1205,4	160	75
P12	Cellular	-	160	80
P13	Cellular	993,7	160	80
P14	Cellular	1360,0	160	80
P15	Cellular	-	160	100
P16	Cellular	943,0	160	100
P17	Cellular	1424,0	160	100

All the sections are made from hot rolled IPE220 steel profiles with 600 [mm] length and in case of the cellular sections the circular holes cut directly from the web, resulting in a section with the same height, differente dimeter, web post and thikness of intumescent coating as represented in the

Table 5, and shown in Figure 29.

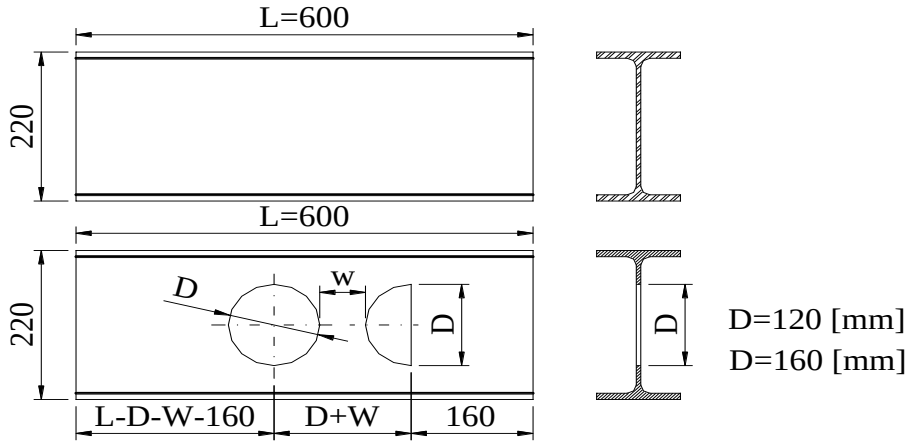

Figure 29: Dimensions of the tested solid and cellular beams.

For the analysis of the steel temperature evolution several thermocouples type K were used as recommended by the standard EN13381-9, [16, 17, 21], positioned and numbered as shown in Figure 30. Two types of type K thermocouples were used, presented in Figure 31. For the case of unprotected beams the thermocouples wires were welded to the steel surface, but for the sections with fire protection, the thermocouples were installed after coating the steel member and mineral insulated thermocouples with Inconel sheath were used by means of a drilled hole of 2 [mm]. By this procedure it was wanted to minimize the influence of the thermocouple wires on the coating expansion and therefore on the fire protection efficiency.

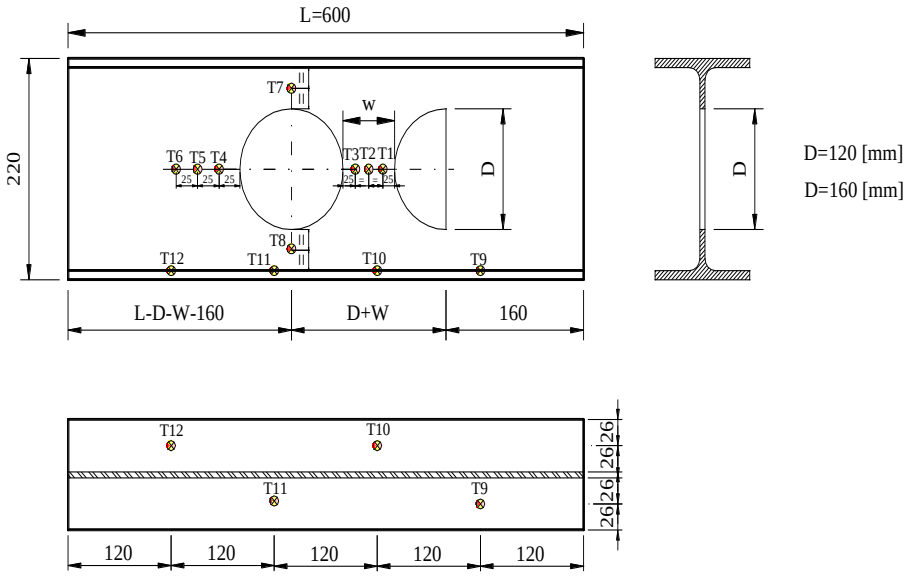

Figure 30: Position and numbering of the thermocouples.

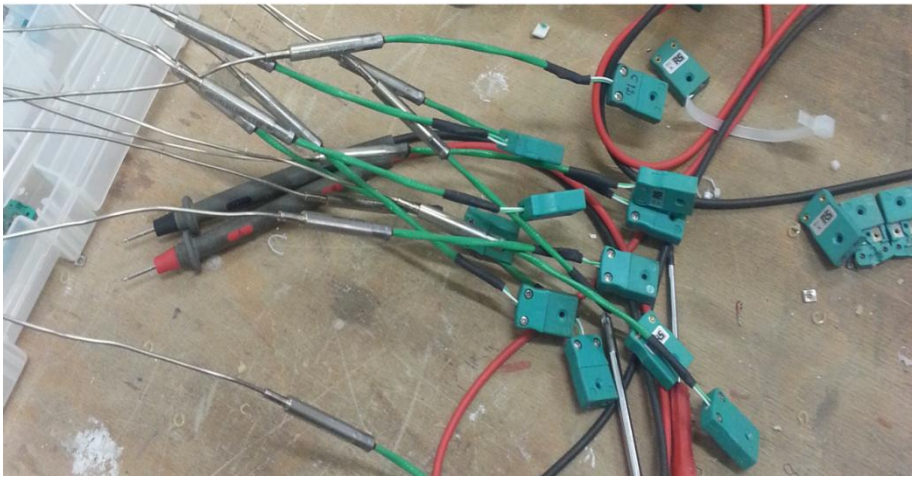

Figure 31: The thermoucouple used in the experimental tests.

The fire resistance tests were performed on a fire furnace with interior dimensions of 1x1x1 [m^3], insulated with refractory bricks and ceramic fibber. It is a gas furnace with four gas burners in which the temperature evolution follows the specifications of the standard EN1363-1, [18], and is controlled by a plate thermocouple represented in Figure 32.

Figure 32: Fire furnace with interior dimensions of 1x1x1 [m^3].

Coating was applied with several coats to achieve the required DFT. The thickness was measured with a dry measuring device on the cross section and several measuring points on the contour, as specified by the standard EN 13381-8,[22].

For the unprotected and protected beams the thermocouples were installed after coating and mineral insulated thermocouples with Inconel sheath were used by means of a drilled hole of 1.5 [mm].

The specimens were placed inside the furnace protected with intumescent coating, with the top flange insulated with ceramic mat in contact with the furnace roof and also with both ends protected, representing an exposure condition from 3 faces, as presented in Figure 34 before the test.

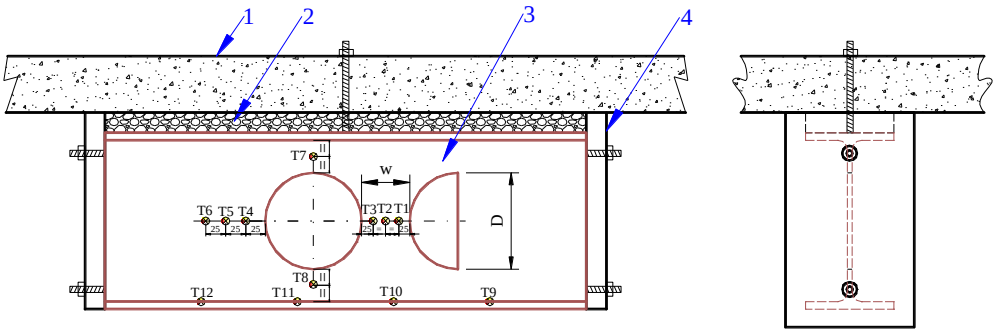

Figure 33: Test setup, position and numbering of the thermocouples.

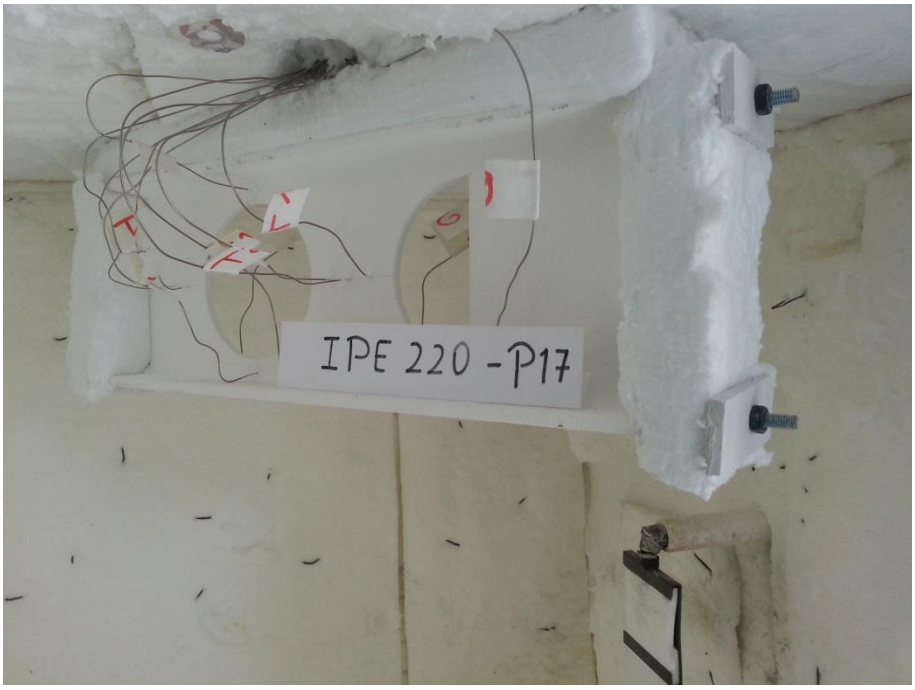

Figure 34: Specimens setup inside the furnace before the test.

Figure 35: Specimen P17 inside the furnace after the test.

Figure 35 presented the same beam after the test with the expansion of the intumescent coating.

The protected and unprotected sections (3) were placed with the top flange fixed to the furnace roof (1) and with a ceramic mat layer of 50 [mm] in-between (2), simulating in all the cases a fire exposure by three sides (4). Also the beams ends were also insulated by an equivalent ceramic mat to avoid the heat transfer from the ends, as can be seen in Figure 36 and Figure 37, for unprotected and protected beams, respectively.

Figure 36 - Tests P12 and P15 before and after the test.

Figure 37 Tests P4 and P3 before and after the test.

3.3 Temperature results of protected and unprotected sections

The steel temperature evolution of the tests was measured by the attached thermocouples. The flange temperature is determined by the thermocouples T9 to T12 and the web post temperatures by the thermocouples T1, T2 and T3. The data obtained from T7 and T8 can be used to verify the non-uniform temperature distribution across the section due to the three side fire exposure. During the test some of the thermocouple temperatures presented some unrealistic fluctuations, possibly due to an intermittent contact to steel and as a consequence were disregarded from the following graphs and analysis.

3.4 Temperature evolution for cellular and solid beams with and without protection:

The temperature evolution for the unprotected solid and cellular beams is presented in Figure 38 and Figure 39, respectively.

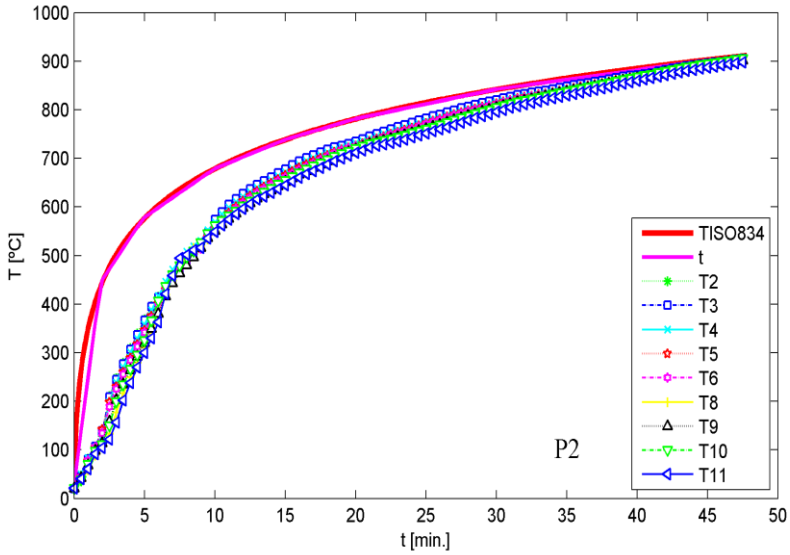

Figure 38: Temperature evolution results of unprotected solid beam P2.

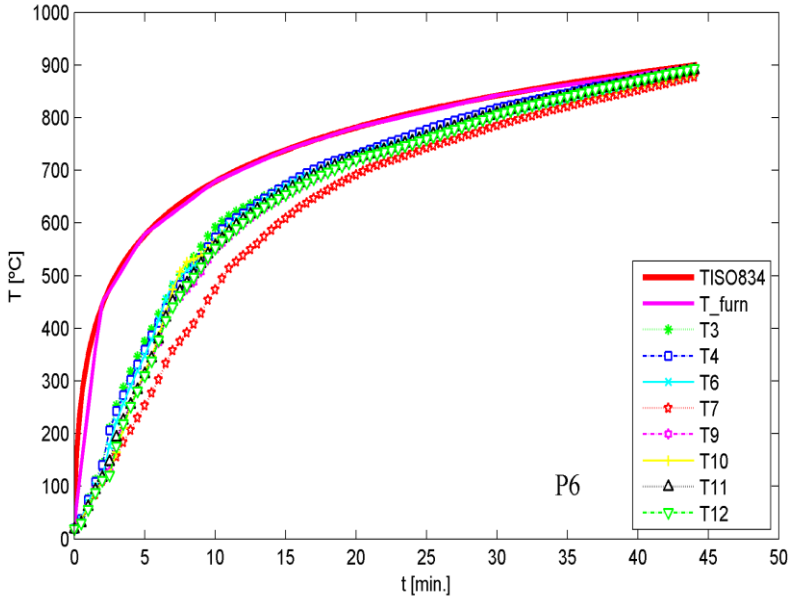

Figure 39: Temperature evolution results of unprotected cellular beam P6.

The results of unprotected solid and cellular beams show for the differente termoucouples for each position in the beam.

Evolution of the average temperature registered on the web post and flanges of test P2 and P6 are presented in the next figures. In both sections the temperature of the cellular beams in smaller than its equivalent solid beams represented in Figure 40 and Figure 41

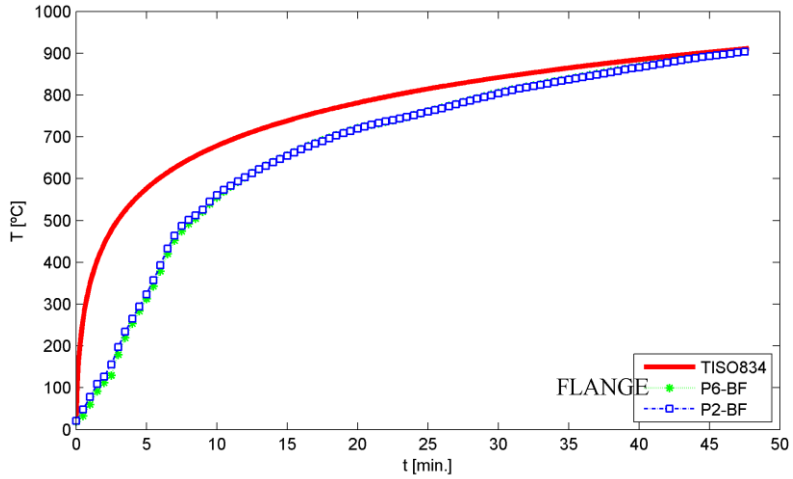

Figure 40: Average temperature on the flange of test P2 and P6.

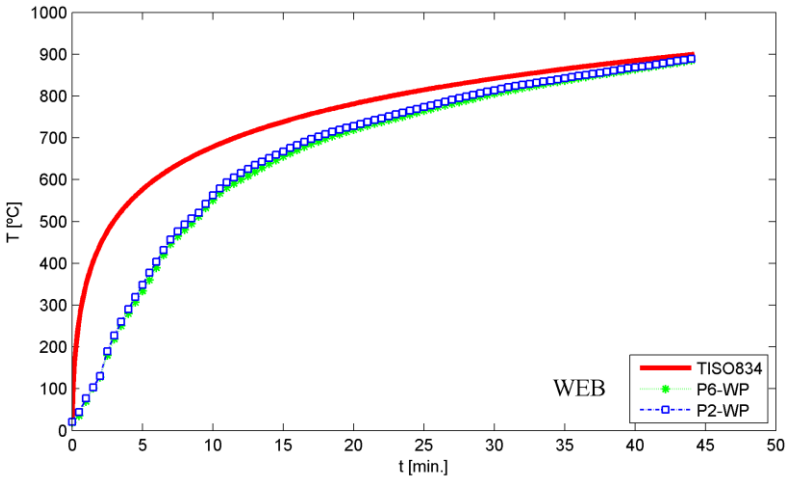

Figure 41: Average temperature on the web of test P2 and P6.

The temperature evolution of the cellular beams with intumescent protection is presented next. For the test P7, with an intumescent coating thikness equal to 860.4[μm] and hole diameter equal to 120 [mm] and a web post equal to 60 [mm], the temperature results are presented in Figure 42.

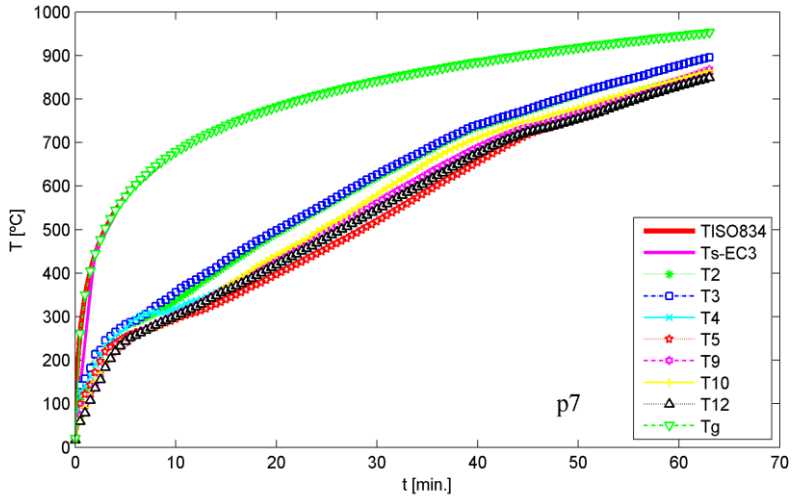

Figure 42: Temperature evolution for test P7.

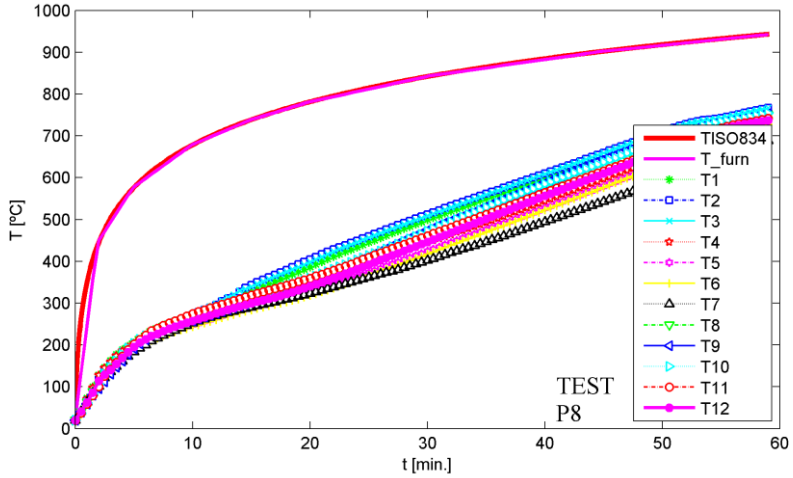

Figure 43: Temperature evolution for test P8.

The experimental results from the fire test made on the specimen P8, is shown in Figure 43, for an intumescent coating equal to 1311 [μm] a hole diameter equal to 120 [mm] and a web post equal to 60 [mm].

In Figure 44 the temperatures curves in each position of the beam P10 is presented. This beam consider a thikness of intumescent coating equal to 960.4[μm] and diameter of hole equal to 120 [mm] also the web post equal to 75 [mm].

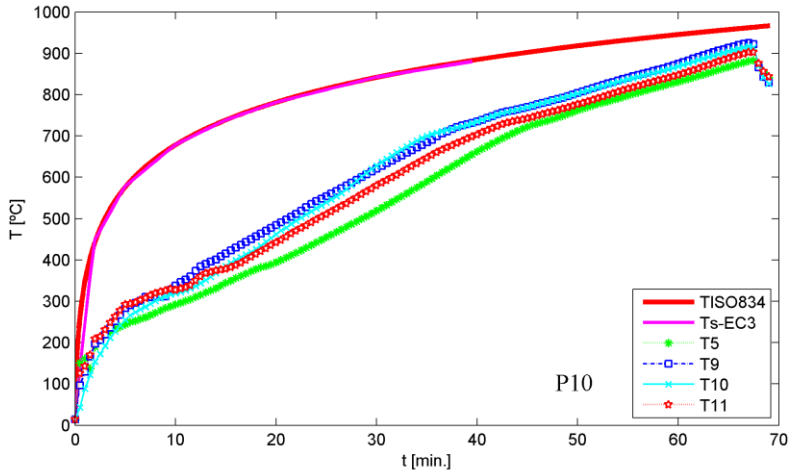

Figure 44: Temperature evolution for test P10.

The test P11, represented in Figure 45, have a thikness of intumescent coating equal to 1205,4 [μm] and diameter of hole equal to 160 [mm] also the web post equal to 75 [mm].

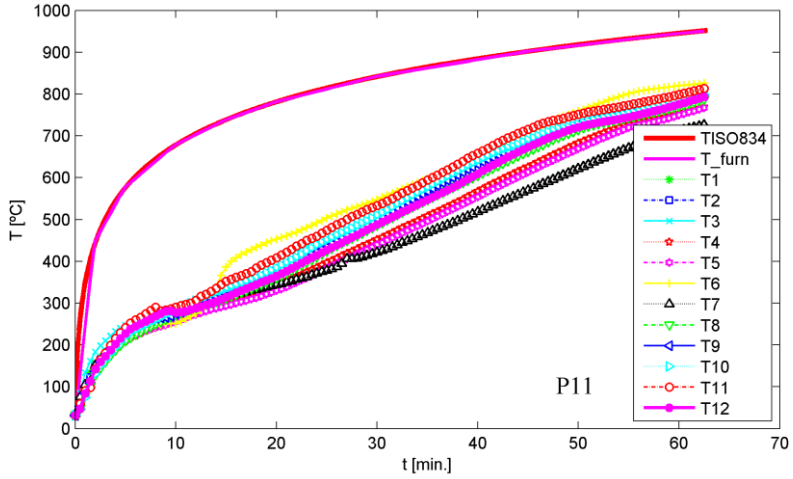

Figure 45: Temperature evolution for test P11.

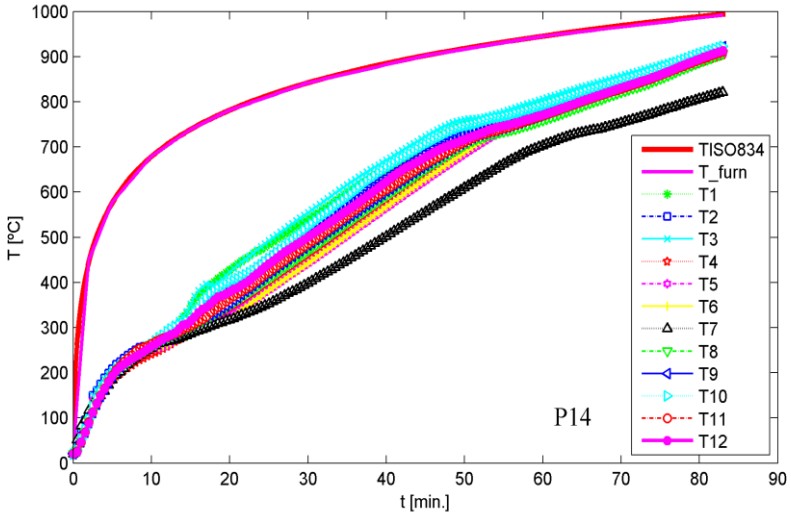

Figure 46: Temperature evolution for test P14.

For the test p14 we have thikness of intumescent coating equal to 1360,4[μm] and diameter of hole equal to 160 [mm] also the web post equal to 80 [mm].In Figure 46 we have differente curve of temperature in each position in the beam.

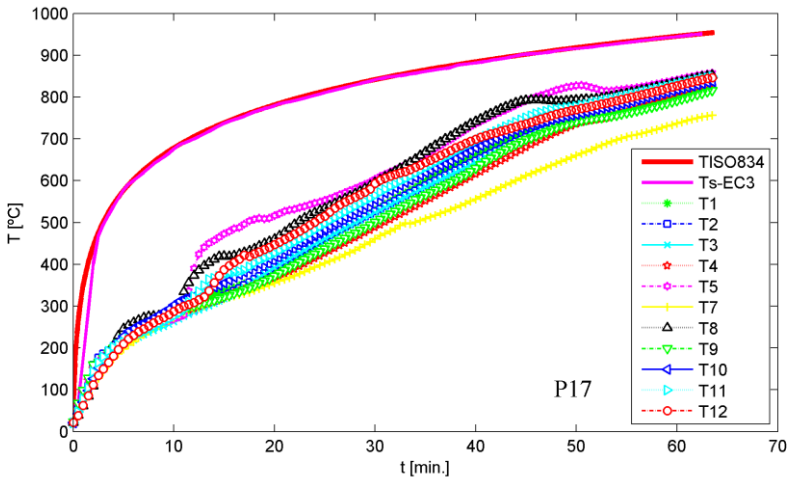

Figure 47: Temperature evolution for test P17.

The results of test p17 are showed in Figure 47 with a thikness of the protection material equal to 1424[μm] and diameter of hole equal to 160 [mm] also the web post equal to 100 [mm].

3.5 Avrage temperature of web and flange for all tests

The average temperature of the web and flange for all experimental tests done are presented in the next figures. The temperature of the cellular beams in smaller than its equivalent solid beam for the flange and the web compared with protected cellular beams, as shown in Figure 48 and Figure 49.

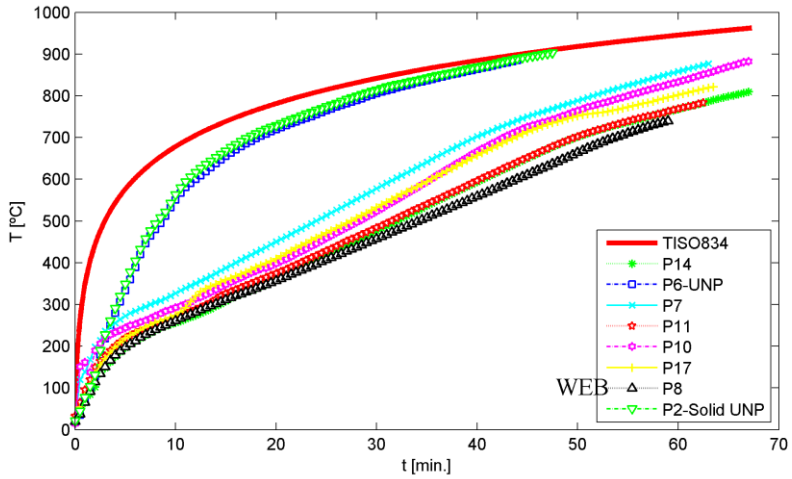

Figure 48: Average temperature of the web post for all beams protected and unprotected.

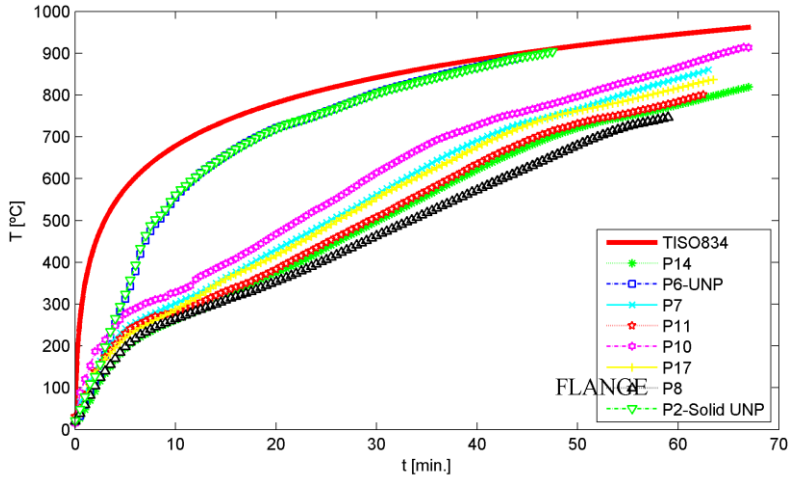

Figure 49: Average temperature of the flange for all beams protected and unprotected.

Table 6 represent the analysis made to the tests results of the solid and cellular beams with and without protection and with different value of DFT, web post and diameter, considering the time to reach a reference temperature of 550 [ºC] and the global average steel temperature after a fire exposure of 30 [min] for all the tests.

Table 6: Average temperature in 30 min and the time to reach 550 [ºC] for all the tests

Ref.	**Beam type**	**DFT [µm]**	**D [mm]**	**W [mm]**	**t (T=550 [ºC]) [min]**	**T (t=30 [min.]) [ºC]**
P1	Solid				11	810,0
P2	Solid	-	-	-	9	812,6
P3	Solid	1047,3	-	-	36	481,7
P4	Solid	1187,5	-	-	49	378,5
P5	Cellular	-	120	60	10	815,7
P6	Cellular	-	120	60	9	805,8
P7	Cellular	860,4	120	60	18	675,6
P8	Cellular	1311,0	120	60	38	461,0
P9	Cellular	-	120	75	11	799,9
P10	Cellular	960,4	120	75	20	655,2
P11	Cellular	1205,4	160	75	34	492,0
P12	Cellular	-	160	80	10	811,9
P13	Cellular	993,7	160	80	28	576,4
P14	Cellular	1360,0	160	80	35	483,5
P15	Cellular	-	160	100	12	792,0
P16	Cellular	943,0	160	100	28	580,3
P17	Cellular	1424,0	160	100	29	562,5

Considering the global average temperature of the beams, the time to reach a temperature of 550 [ºC] is 10 minutes for P6, but for P7 and P8 the time increases significantly to 18 minutes and 38 minutes respectively, as presented in

Table 6.

The effects of the used of the fire protection material can be seen from the comparison betweed P6 and P7. Test P6 without protection and has a time to reach 550 [ºC] equal 9 minutes. When a fire protection is used, like the test P7 with DFT equal to 860.4 [μm] we can obtain an increase in the time to reach a temperature 550[ºC] to 18 minutes. The temperature after 30 minutes of fire exposure leads to a decrease of the steel temperature to 675,58 [ºC]. Increasing the DFT to 1311[μm], using the example from P8, a time increase is obtained to 38 minutes and a decrease of temperature to 461 [ºC].

The structural behavior of the cellular beam is influenced by the web opening size. The decreases of the temperature in protected cellular beams due to the increase of opening size, the increases of the web post also affect a increasing of temperature in cellular beam.

The intumescent coating expansion of the cellular beams P17 and P14, protected with a nominal DFT equal to 1424, 0 and 1360, 0 [mm], measured at the web post is equal to 30 [mm]. The state of the beams at the test end is shown in Figure 50 and Figure 51.

The intumescent coating expansion of the cellular beams P10 , P8 and P11, protected with a nominal DFT around 1000 [mm], measured at the web post ranges from 20-25 [mm] showed in Figure 52, Figure 53 and Figure 54.

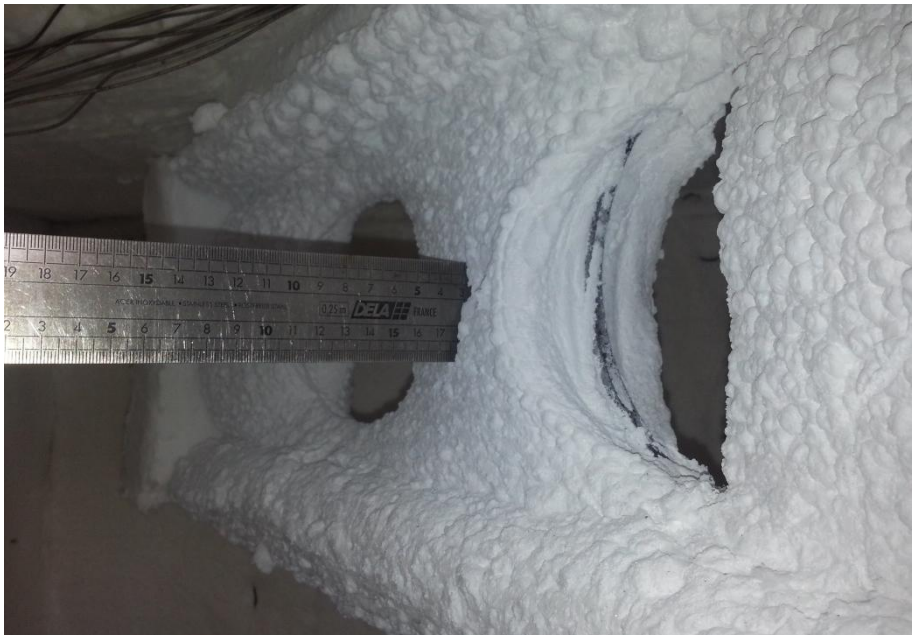

Figure 50: Measured expansion of intumescent char for test P17.

Figure 51: Measured expansion of intumescent char for test P14

Figure 52: Measured expansion of intumescent char for test P8

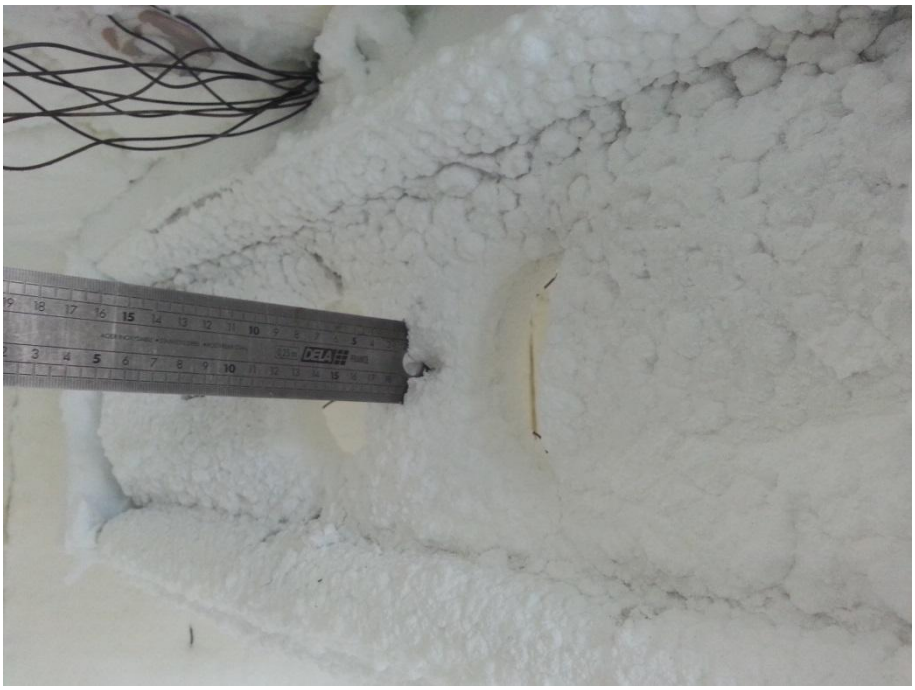

Figure 53: Measured expansion of intumescent char for test P10

Figure 54: Measured expansion of intumescent char for test P11.

Chapter 4: Conclusions and Future Work

4.1 Main conclusions

The aim of this work was to investigate the efficiency of intumescent coating, designed for the protection of steel in the event of a fire by doing experimental tests on protected and unprotected solid and cellular beams subjected to a fire exposure on three sides. The effects of flame retardant components on the performance of intumescent coatings in terms of sticking ability, fire protection, thermal degradation and stability,. The parametric analysis allows comparing the performance of an intumescent coating as a fire protection material using beams with and without intumescent protection. Additionally, it is also studied the effect of intumescent thickness, the hole diameter and the web post width in the case of cellular beams.

This work done with reference to the standards EN13381-8 for solid beams protected with intumescent paint and EN13381-9 for the analysis of cellular beams protected with intumescent paint.

The experimental temperature results show intumescent coating efficiency when applied to solid beams and also for cellular beams, resulting from its application an increase fire the re-sistance time in both cases. Considering for example the time required for the steel to reach 550 [ºC], solid beam without protection time of 9 minutes, while for cellular beams with a hole diameter of 120[mm] and nominal thinkness of 860,4 [μm]the increase is equal to 18 minutesand with more protection of 1311,0 [μm]and the same diameter the increase is equal to 38 minute.

For the test in cellular beams with web posts of 80 and 100[mm] do not show any sig-nificate temperature difference neither in relation to the fire resistance time. For both beams, when is applied a nominal DFT equal to 1000 [μm], the temperature of 550 [ºC] is

achieved after 10 minutes and 12 minute respectivly. For longer fire exposure periods a slight difference can be already verified.

For the case of a cellular beam with intumescent coating, we conclude a small contraction of the intumescent char around the circular hole, leaving a small area of steel directly exposed to fire and this because of higher temperature and the thikness of the coating.

4.2 Future lines of investigation

In future research can be developed further for cellular beam having more tests with intumescent coating with differente geometries of the beam compared with numrical method (ANSYS).

This study need more experimental test about the behaviour of cellular beam in elevated temperature submited with thermal and mechanical load, also with differente section cellular beam and differente web post, diameter, and hight of the beam.

References

[1]. Bailey, C., *Indicative fire tests to investigate the behaviour of cellular beams protected with intumescent coatings.* Fire Safety Journal, 2004. **39**(8): p. 689-709.

[2]. G. Bihina a, B.Z., A. Bouchaïr b, *Behaviour of composite steel–concrete cellular beams in fir.* (2013. **2217–2228**.

[3]. Wang, P., et al., *Web-post buckling of fully and partially protected cellular steel beams at elevated temperatures in a fire.* Thin-Walled Structures, 2016. **98, Part A**: p. 29-38.

[4]. Guo-Qiang Li a, J.H., n, Guo-Biao Lou a, Yong C. Wang, *Predicting intumescent coating protected steel temperature in fire using constant thermal conductivity.* Thin-Walled Structures, 2016. **177–184**.

[5]. Nadjai, A., et al., *Performance of unprotected and protected cellular beams in fire conditions.* Construction and Building Materials, 2016. **105**: p. 579-588.

[6]. Bailey, K.C.G., *Temperature distribution of intumescent coated steel framed connection at elevated temperature.* 2009. **8**(University of Manchester, UK): p. 8.

[7]. Bake, S., *Behaviour of cellular beams and cellular composite floors at ambient and elevated temperatures*, in *civil engenniring*. 2010, Manchester UK. p. 260.

[8]. Protection, A.f.S.F., *Fire protection for structural steel in buildings*. June 2004.: 2004. 162.

[9]. Delphine Sonck , J.B., *Lateral–torsional buckling resistance of cellular beams.* Journal of Constructional Steel Research, 2015. **105** p. 119–128.

[10]. Luis Mesquita, J.G., Gustavo Gonçalves, Paulo Piloto, Kada Abdelhak, *INTUMESCENT FIRE PROTECTION OF CELLULAR BEAMS.* 2015.

[11]. Jean-Marc Franssen, V.K., Raul Zaharia., *Designing Steel Structures for Fire Safety*. 2009. 158.

[12]. CEN, *EN1991-1-2 Eurocode 1: Actions on Structures, Part 1.2: General Actions, Actions on Structures Exposed to Fire.* 2002, European Committee for Standardization: Brussels, Belgium.

[13]. Wickstrom, U., *Comments on calculation of temperature in fire exposed bare steel structures in prEN 1993-1-2: Eurocode 3—design of steel structures—Part 1–2: general rules—structural fire design,Fire Safety Journal 40 .191-192, 2005*

[14]. Franssen, J.-M., *Calculation of temperature in fire-exposed bare steel structures:Comparison between ENV 1993-1-2 and EN 1993-1-2.* Fire Safety Journal 41, 2006: p. 139–143.

[16]. CEN, *ENV1993-1-2, Eurocode 3: Design of Steel Structures, Part 1-2: General rules, Structural fire design*. 1995, European Committee for Standardization: Brussels, Belgium.

[17]. *CEN, EN 13381-9: Test methods for determining the contribution to the fire resistance of structural members Part 9: Contribution of fire resistance to steel*

beams with web opening. 2015, European Committee for Standardization: European Committee for StandardizationBrussels, Belgium., 2015.

[18]. *Test methods for determining the contribution to the fire resistance of structural members — Part 9: Applied fire protection systems to steel beams with web openings.* 2012(EN 13381-9:2012).

[19]. *CEN, EN1363-1: Fire resistance tests. General requirements.* . European Committee for Standardization: Brussels, Belgium., 2012,.

[20]. Chian, Y.M., *investigation on water-borne intumescent fire protective coatings for steel* 2011, MALAYA.

[21]. A. P. Mouritz, A.G.G., *Fire Properties of Polymer Composite Materials*. Vol. 143. 2006. 401.

[22]. *Test methods for determining the contribution to the fire resistance of structural members Part 8: Applied reactive protection to steel members*. april 2010: European Standart.

Annex

A1. Publications

[1] Brahim Lamri, Luís Mesquita, Abdelhak Kada, Paulo Piloto; BEHAVIOUR OF CELLULAR BEAMS PROTECTED WITH INTUMESCENT COATINGS, 5th workshop on Urban fires Safety, Laboratório Nacional de Engenharia Civil (LNEC), Lisboa, Portugal, 1-2 Junho de 2016.

A2. MATLAB PROGRAM FOR UNPROTECTED SOLID AND CELLULAR BEAMS

```
function [Ta]=EC3Part12
clc
clear all
close all
%   Datas
% Ksh : correctlon factor for the shadow effect
% Am/V : the section factor for unprotected steel members [l/m];
% Am : the surface area of the member per unit length [m2/m];
% V : the volume of the member per unit length [m3/m];
% Ca : the specific heat of steel, [J/kgK];
% dothnetd : the design value of the net heat flux per unit area [W/m2];
% Dt : the time interval [seconds];
% roa : the unit mass of steel [kg/m3]
% Tg : gas temperature in the fire compartment [°C]
%     (Effective radiation temperature of the fire environment)
% Ta1 : Surface temperature of the member of Unprotected steel 4 faces exposed
(°C)
% Ta2 : Surface temperature of the member  of Unprotected steel 3 faces exposed
(°C)
% t, t1 : Time (in sec)
% Dt : the time interval (sec)

% L : Length of Beam
L=0.6       % Length of Beam (m)

% Profile of beam
disp([ '************************************' ])
disp([ 'The profile of beam is :' ])
disp([ 'For IPE220:    Type 1' ])
disp([ 'For IPE160:    Type 2' ])
disp([ 'For IPE200:    Type 3' ])
disp([ 'For IPE300:    Type 4' ])
disp([ 'For IPE500:    Type 5' ])
disp([ 'For HEB100:    Type 6' ])
disp([ 'For HEB160:    Type 7' ])
disp([ 'For HEB200:    Type 8' ])
disp([ 'For HEB300:    Type 9' ])
disp([ '************************************' ])
Profile = input('Select the profile  ');

switch Profile
   case 1,
```

```
% Geometry IPE 220
h=0.22; % h=220 mm            Heigh of section IPE
b=0.11; % b=110 mm            Width of section IPE
tw=0.0059; % tw=5.9 mm        Thickness of web
tf=0.0092; % tf=9.2 mm        Thickness of flange
r=0.012; % r=12 mm            Radius
A=33.4E-4; % A=33.4 cm2       Area of section IPE
nh=1.5        %nh= Number of holes

namep1='IPE100-4SidesCB';
namep2='IPE100-3SidesCB';
namep3='IPE100-4SidesSB';
namep4='IPE100-3SidesSB';
namep='IPE100';
case 2,
% Geometry IPE 160
h=0.16; % h=160 mm            Heigh of section IPE
b=0.082; % b=82 mm            Width of section IPE
tw=0.005; % tw=5 mm           Thickness of web
tf=0.0074; % tf=7.4 mm        Thickness of flange
r=0.009; % r=9 mm            Radius
A=20.1E-4; % A=20.1 cm2       Area of section IPE
nh=((L+0.714*h)/(1.5*0.714*h))-1 ;        %nh= Number of holes
nh=floor(nh);
namep1='IPE160-4SidesCB';
namep2='IPE160-3SidesCB';
namep3='IPE160-4SidesSB';
namep4='IPE160-3SidesSB';
namep='IPE160';
case 3,
% Geometry IPE 200
h=0.2; % h=200 mm             Heigh of section IPE
b=0.1; % b=100 mm             Width of section IPE
tw=0.0056; % tw=5.6 mm        Thick of web
tf=0.0085; % tf=8.5 mm        Thickness of flange
r=0.012; % r=12 mm            Radius
A=28.5E-4; % A=28.5 cm2       Area of section IPE
nh=((L+0.714*h)/(1.5*0.714*h))-1  ;       %nh= Number of holes
nh=floor(nh);
namep1='IPE200-4SidesCB';
namep2='IPE200-3SidesCB';
namep3='IPE200-4SidesSB';
namep4='IPE200-3SidesSB';
namep='IPE200';
case 4,
% Geometry IPE 300
h=0.3; % h=300 mm             Heigh of section IPE
```

```
b=0.15; % b=150 mm            Width of section IPE
tw=0.0071; % tw=7.1 mm        Thickness of web
tf=0.0107; % tf=10.7 mm       Thickness of flange
r=0.015; % r=15 mm            Radius
A=53.8E-4; % A=53.8 cm2       Area of section IPE
nh=((L+0.714*h)/(1.5*0.714*h))-1 ;        %nh= Number of holes
nh=floor(nh);
namep1='IPE300-4SidesCB';
namep2='IPE300-3SidesCB';
namep3='IPE300-4SidesSB';
namep4='IPE300-3SidesSB';
namep='IPE300';
case 5,
% Geometry IPE 500
h=0.5; % h=500 mm             Heigh of section IPE
b=0.2; % b=200 mm             Width of section IPE
tw=0.0102; % tw=10.2 mm       Thick of web
tf=0.0057; % tf=5.7 mm        Thickness of flange
r=0.021; % r=21 mm            Radius
A=115.5E-4; % A=115.5 cm2      Area of section IPE
nh=((L+0.714*h)/(1.5*0.714*h))-1        %nh= Number of holes
nh=floor(nh);
namep1='IPE500-4SidesCB';
namep2='IPE500-3SidesCB';
namep3='IPE500-4SidesSB';
namep4='IPE500-3SidesSB';
namep='IPE500';
case 6,
% Geometry HEB 100
h=0.1; % h=100 mm             Heigh of section IPE
b=0.1; % b=100 mm             Width of section IPE
tw=0.006; % tw=6 mm          Thickness of web
tf=0.010 ; % tf=10 mm        Thickness of flange
r=0.012; % r=12 mm            Radius
A=26E-4; % A=26 cm2       Area of section IPE
nh=((L+0.714*h)/(1.5*0.714*h))-1  ;       %nh= Number of holes
nh=floor(nh);
namep1='HEB100-P4SidesCB';
namep2='HEB100-P3SidesCB';
namep3='HEB100-4SidesSB';
namep4='HEB100-3SidesSB';
namep='HEB100';
case 7,
% Geometry HEB160
h=0.16; % h=160 mm            Heigh of section IPE
b=0.16; % b=160 mm            Width of section IPE
tw=0.008; % tw=8 mm          Thickness of web
```

```
   tf=0.013 ; % tf=13 mm        Thickness of flange
   r=0.015; % r=15 mm           Radius
   A=54.3E-4; % A=54.3 cm2      Area of section IPE
   nh=((L+0.714*h)/(1.5*0.714*h))-1;        %nh= Number of holes
   nh=floor(nh);
   namep1='HEB160-P4SidesCB';
   namep2='HEB160-P3SidesCB';
   namep3='HEB160-4SidesSB';
   namep4='HEB160-3SidesSB';
   namep='HEB160';
   case 8,
   % Geometry HEB 200
   h=0.2; % h=200 mm            Heigh of section IPE
   b=0.2; % b=200 mm           Width of section IPE
   tw=0.009; % tw=9 mm         Thickness of web
   tf=0.015 ; % tf=15 mm       Thickness of flange
   r=0.018; % r=18 mm           Radius
   A=78.1E-4; % A=78.1 cm2      Area of section IPE
   nh=((L+0.714*h)/(1.5*0.714*h))-1   ;      %nh= Number of holes
   nh=floor(nh);
   namep1='HEB200-P4SidesCB';
   namep2='HEB200-P3SidesCB';
   namep3='HEB200-4SidesSB';
   namep4='HEB200-3SidesSB';
   namep='HEB200';
   case 9,
   % Geometry HEB 300
   h=0.3; % h=300 mm            Heigh of section IPE
   b=0.3; % b=300 mm           Width of section IPE
   tw=0.011; % tw=11 mm        Thickness of web
   tf=0.019 ; % tf=19 mm       Thickness of flange
   r=0.027; % r=27 mm           Radius
   A=149.1E-4; % A=149.1 cm2      Area of section IPE
   nh=((L+0.714*h)/(1.5*0.714*h))-1 ;        %nh= Number of holes
   nh=floor(nh);
   namep1='HEB300-P4SidesCB';
   namep2='HEB300-P3SidesCB';
   namep3='HEB300-4SidesSB';
   namep4='HEB300-3SidesSB';
   namep='HEB300';

   otherwise
   return;
   %séquence d'instructions par défaut
end
%
% Beam with circle Holes
```

```
D=0.714*h                % Diameter of hole
rh=D/2 ;                 %  Radius of  hole
Ah=pi*rh^2 ;             % Area of a hole
Hp= 2*pi*rh ;            % Perimeter of a hole
%
% Characteristics of material
roa=7850; % roa=7850 kg/m3   % density of steel
phi=1;                   % Configuration factor
alphac=25;               % Coefficient of heat transfer by convection
epsm=0.7;                % Surface emissivity of the member
epsf=1;                  % Emissivity of flames, of the fire
%
boltz=5.67e-8;           % Stephan Boltzmann constant (=5,67×10-8 [W/m2K4])
%
% For Unprotected internal steelwork exposed in 4 sides (Cellular beam)
Am1=(4*b+2*(h-tw-4*r)+2*pi*r)-nh*Ah*2+nh*Hp*tw      ; % for 4 sides
V=A*L-nh*Ah*tw;
AmV1=Am1/V; AmVb1=2*(h+b)/A;% for 4 sides
ksh1=0.9*AmVb1/AmV1; % for 4 sides


% For Unprotected internal steelwork exposed in 3 sides (Cellular beam)
Am2=(3*b+2*(h-tw-4*r)+2*pi*r)-nh*Ah*2+nh*Hp*tw ; % for 3 sides
V=A*L-nh*Ah*tw;
AmV2=Am2/V; AmVb2=(2*h+b)/A; % for 3 sides
ksh2=0.9*AmVb2/AmV2;         % for 3 sides

%ForUnprotected internal steelwork exposed in 4 sides (Solid beam)
Am3=4*b+2*(h-tw-4*r)+2*pi*r; % for 4 sides
V=A;
AmV3=Am3/V; AmVb3=2*(h+b)/A;% for 4 sides
ksh3=0.9*AmVb3/AmV3; % for 4 sides
kAmV=ksh3*AmV3;

% For Unprotected internal steelwork exposed in 3 sides(Solid beam)
Am4=3*b+2*(h-tw-4*r)+2*pi*r; % for 3 sides
V=A;
AmV4=Am4/V; AmVb4=(2*h+b)/A;% for 3 sides
ksh4=0.9*AmVb4/AmV4; % for 3 sides

% section factor for the web
Am5=(2*h)-(4*tf);
V5=(h-2*tf)*tw;
AmV5=Am5/V5;

% section factor for the flange
Am6=(2*b + 2*tf)- tw;
```

```
V6=b*tf ;
AmV6=Am6/V6;
% vector data
%ksh_vect=[ksh1 ksh2 ksh3 ksh4 1 1];
ksh_vect=[1 1 1 1 1 1];
AmV_vect=[AmV1 AmV2 AmV3 AmV4 AmV5 AmV6];
AmV1;
AmV3;

ksh1*AmV1;
ksh3*AmV3;

Dt=1;  % in seconds

tfinal=7201;
% dothnetd1 : exposed to fire on 4 sides
% dothnetd2 : exposed to fire on 3 sides
for j=1:length(AmV_vect)
   i=1;
   t=0;
   time(i)=t;
   Ta(i,j)=20;   Tg(i,j)=20;
   ksh=ksh_vect(j);
   AmV=AmV_vect(j);
% Section of Steel exposed to fire on 4 and 3 sides
for i=2:tfinal
   t=t+Dt;
   time(i)=t;
   Tg(i,j)=20+345*log10(8*t/60+1);
   param1=boltz*phi*epsm*epsf;
 dothnetd1=param1*((Tg(i,j)+273)^4-(Ta(i-1,j)+273)^4)+alphac*(Tg(i,j)-Ta(i-1,j));

   Ca=prop_ca(Ta(i-1,j));
   DTst=ksh*((AmV)/(Ca*roa))*dothnetd1*Dt; % temp calculqtion
   Ta(i,j)=DTst+Ta(i-1,j)  ;

end
interp_time=[0:60:tfinal];
temp_interp(:,j)=linterp(time,Ta(:,j),interp_time);

%format shortg
%ref_temp=[500 600];
%ref_time(:,j)=linterp(Ta(:,j),time,ref_temp);


%ref_time2=60*[15 30];
%ref_temp2(:,j)=linterp(time,Ta(:,j),ref_time2);
```

```
        %%%%%%%%%%%%%%%%%%%%%%%%%%%%%%%%%%%%%%%%%%%%%%%%%%%%%%%%%%%%%%%%%%%%%%%%%%%%%
        end


        %figure1=figure()

        colors_lines='kgbcrmykgbcrmy';
        lines1={'-';':';'-.';'-';':';'-.';'-';':';'-.';'-';':';'-.';'-';':';'-.';'-';':';'-.';'-';':';'-.';'-';':';'-.';'-';':';'-.';'-';':';'-.';'-';':';'-.';'-';':';'-.'};
        marks='o*sph+^v<>o';
        figuresize=[0 0 19 9*19/16];% FIGURE SIZE IN CENTIMETERS ASPECT RATIO 4:3
        figure1 = figure('Units','centimeters','Color',[1 1 1], 'Position',figuresize);

        plot(time,Tg(:,2),'r','LineWidth',2)
        hold on;
        for j=1:length(AmV_vect)

        plot(interp_time,temp_interp(:,j),'LineStyle',lines1{j},'LineWidth',1,'Color',colors_lines(j),'Marker', marks(j),'MarkerSize',3)
        hold on;
        end
        axis([0 900 0 1000]);
        xlabel('t [s]');
        ylabel('T [°C]');
        %title('Evolution of the temperature vs time (unprotected steel elements)')
        %title('Unprotected Cellular beam and Solid beam')
        legend('ISO 834',namep1,namep2,namep3,namep4,'Web','flange','Location','southeast')
        filename=strcat(namep,'.png')

        set(gcf, 'PaperPositionMode', 'auto');
        print('-dpng','-r200',filename)

        %print(figure1,'-r300','-dpng',filename)
        end
        % material properties
        function Ca=prop_ca(T);
        Ta=T;
          if and(Ta<600,Ta>=20)
              Ca=425+7.73e-1*Ta-1.69e-3*Ta^2+2.22e-6*Ta^3;
            elseif and (Ta<735,Ta>=600)
              Ca=666+13002/(738-Ta);
            elseif and (Ta<900,Ta>=735)
              Ca=545+17820/(Ta-731);
```

```
    elseif and (Ta<1200,Ta>=900)
        Ca=650;
    end;
end
```

A3. MATLAB PROGRAM FOR PROTECTED SOLID AND CELLULAR BEAMS

```
function EC3Part12SSF
clc
clear all
close all
%%%%%%%%%%%%%%%%%%%%%%%%%%%%%%%%%%%%%%%%%%%%%%%%
%%%%%%%%%%%%%%%%%   Datas
% Ksh : correctlon factor for the shadow effect
% Am/V : the section factor for unprotected steel members [l/m];
% Am : the surface area of the member per unit length [m2/m];
% V : the volume of the member per unit length [m3/m];
% Ap/V : the section factor for protected members [l/m];
% Ap : the appropriate area of firc protection material per unit length of the member
[m2/m]
% Ca : the specific heat of steel, [J/kgK];
% Cp : the specific heat of protection material, [J/kgK];
% dothnetd : the design value of the net heat flux per unit area [W/m2];
% Dt : the time interval [seconds];
% rhoa : the unit mass of steel [kg/m3]
% rhop : the unit mass of protection material [kg/m3]
% Tg : gas temperature in the fire compartment [°C]
%     (Effective radiation temperature of the fire environment)
% Ta1 : Surface temperature of the member of Unprotected steel 4 faces exposed (°C)
% Ta2 : Surface temperature of the member  of Unprotected steel 3 faces exposed (°C)
% t, t1 : Time (in sec)
% dp : Thickness of protection material
% kp : Thermal Conductivity of protection material

% L : Length of Beam
L=1;        % Length of Beam (m)

% Profile of beam
disp([ '***********************************' ])
disp([ 'The profile of beam is :' ])
disp([ 'For IPE100:    Type 1' ])
disp([ 'For IPE160:    Type 2' ])
disp([ 'For IPE200:    Type 3' ])
disp([ 'For IPE300:    Type 4' ])
disp([ 'For IPE500:    Type 5' ])
disp([ 'For HEB100:    Type 6' ])
disp([ 'For HEB160:    Type 7' ])
disp([ 'For HEB200:    Type 8' ])
disp([ 'For HEB300:    Type 9' ])
disp([ '***********************************' ])
Profile = input('Select the profile  ');
```

```
switch Profile
    case 1,
    % Geometry IPE 100
    h=0.1; % h=100 mm            Heigh of section IPE
    b=0.055; % b=55 mm            Width of section IPE
    tw=0.0041; % tw=4.1 mm        Thickness of web
    tf=0.0057; % tf=5.7 mm        Thickness of flange
    r=0.007; % r=7 mm            Radius
    A=10.3E-4; % A=10.3 cm2      Area of section IPE
     nh=((L+0.714*h)/(1.5*0.714*h))-1 ;        %nh= Number of holes
    nh=floor(nh);
    namep1='IPE100-P4SidesB';
    namep2='IPE100-P3SidesB';
    namep='IPE100';
    case 2,
    % Geometry IPE 160
    h=0.16; % h=160 mm            Heigh of section IPE
    b=0.082; % b=82 mm            Width of section IPE
    tw=0.005; % tw=5 mm           Thickness of web
    tf=0.0074; % tf=7.4 mm        Thickness of flange
    r=0.009; % r=9 mm            Radius
    A=20.1E-4; % A=20.1 cm2      Area of section IPE
     nh=((L+0.714*h)/(1.5*0.714*h))-1 ;        %nh= Number of holes
    nh=floor(nh);
    namep1='IPE160-P4SidesB';
    namep2='IPE160-P3SidesB';
    namep='IPE160';
    case 3,
    % Geometry IPE 200
    h=0.2; % h=200 mm            Heigh of section IPE
    b=0.1; % b=100 mm            Width of section IPE
    tw=0.0056; % tw=5.6 mm       Thick of web
    tf=0.0085; % tf=8.5 mm       Thickness of flange
    r=0.012; % r=12 mm           Radius
    A=28.5E-4; % A=28.5 cm2      Area of section IPE
    namep1='IPE200-P4SidesB';
    namep2='IPE200-P3SidesB';
    namep='IPE200';
    case 4,
    % Geometry IPE 300
    h=0.3; % h=300 mm            Heigh of section IPE
    b=0.15; % b=150 mm           Width of section IPE
    tw=0.0071; % tw=7.1 mm       Thickness of web
    tf=0.0107; % tf=10.7 mm      Thickness of flange
    r=0.015; % r=15 mm           Radius
    A=53.8E-4; % A=53.8 cm2      Area of section IPE
```

```
 nh=((L+0.714*h)/(1.5*0.714*h))-1 ;        %nh= Number of holes
nh=floor(nh);
namep1='IPE300-P4SidesB';
namep2='IPE300-P3SidesB';
namep='IPE300';
case 5,
% Geometry IPE 500
h=0.5; % h=500 mm             Heigh of section IPE
b=0.2; % b=200 mm             Width of section IPE
tw=0.0102; % tw=10.2 mm       Thick of web
tf=0.0057; % tf=5.7 mm        Thickness of flange
r=0.021; % r=21 mm            Radius
A=115.5E-4; % A=115.5 cm2     Area of section IPE
namep1='IPE500-P4SidesB';
namep2='IPE500-P3SidesB';
namep='IPE500';
case 6,
% Geometry HEB 100
h=0.1; % h=100 mm             Heigh of section HEB
b=0.1; % b=100 mm             Width of section HEB
tw=0.006; % tw=6 mm          Thickness of web
tf=0.010 ; % tf=10 mm        Thickness of flange
r=0.012; % r=12 mm            Radius
A=26E-4; % A=26 cm2          Area of section HEB
 nh=((L+0.714*h)/(1.5*0.714*h))-1 ;        %nh= Number of holes
nh=floor(nh);
namep1='HEB100-P4SidesB';
namep2='HEB100-P3SidesB';
namep='HEB100';
case 7,
% Geometry HEB160
h=0.16; % h=160 mm             Heigh of section HEB
b=0.16; % b=160 mm             Width of section HEB
tw=0.008; % tw=8 mm          Thickness of web
tf=0.013 ; % tf=13 mm        Thickness of flange
r=0.015; % r=15 mm            Radius
A=54.3E-4; % A=54.3 cm2       Area of section HEB
 nh=((L+0.714*h)/(1.5*0.714*h))-1 ;        %nh= Number of holes
nh=floor(nh);
namep1='HEB160-P4SidesB';
namep2='HEB160-P3SidesB';
namep='HEB160';
case 8,
% Geometry HEB 200
h=0.2; % h=200 mm             Heigh of section HEB
b=0.2; % b=200 mm             Width of section HEB
tw=0.009; % tw=9 mm          Thickness of web
```

```
   tf=0.015 ; % tf=15 mm         Thickness of flange
   r=0.018; % r=18 mm            Radius
   A=78.1E-4; % A=78.1 cm2       Area of section HEB
    nh=((L+0.714*h)/(1.5*0.714*h))-1 ;        %nh= Number of holes
   nh=floor(nh);
   namep1='HEB200-P4SidesB';
   namep2='HEB200-P3SidesB';
   namep='HEB200';
   case 9,
   % Geometry HEB 300
   h=0.3; % h=300 mm             Heigh of section HEB
   b=0.3; % b=300 mm            Width of section HEB
   tw=0.011; % tw=11 mm         Thickness of web
   tf=0.019 ; % tf=19 mm        Thickness of flange
   r=0.027; % r=27 mm            Radius
   A=149.1E-4; % A=149.1 cm2     Area of section HEB
    nh=((L+0.714*h)/(1.5*0.714*h))-1 ;        %nh= Number of holes
   nh=floor(nh);
   namep1='HEB300-P4SidesB';
   namep2='HEB300-P3SidesB';
   namep='HEB300';

   otherwise
   return;
   %séquence d'instructions par défaut
end

%
% Characteristics of material
rhoa=7850; % roa=7850 kg/m3   % density of steel
phi=1;                    % Configuration factor
alphac=25;                % Coefficient of heat transfer by convection
epsm=0.7;                 % Surface emissivity of the member
epsf=1;                   % Emissivity of flames, of the fire

% Protection material
disp([ '************************************' ])
disp([ 'For Gypsum boards:        Type 1' ]);
disp([ 'For Concrete:             Type 2' ]);
disp([ 'For Light weight concrete: Type 3' ]);
disp([ 'Brick with holes:         Type 4' ]);
disp([ '************************************' ])
Prot = input('Select the protection : ');

switch Prot
   case 1,
   % Characteristics of protection material (Gypsum boards)
```

```
    dp=0.023;              % dp = 23 mm
    rhop=800;              % rhop = 800 kg/m3
    Cp=1700;               % Cp = 1700 J/kg°K
    kp=0.2;               % kp = 0.2 W/m°K
    mc=0.2                 % mc = 20% (Moisture content)
   case 2,
% Characteristics of protection material (Concrete)
    dp=0.020;              % dp = 20 mm
    rhop=2300;             % rhop = 2300 kg/m3
    Cp=1000;               % Cp = 1000 J/kg°K
    kp=1.6;               % kp = 1.6 W/m°K
    mc=0.04;               % mc = 4% (Moisture content)
   case 3,
% Characteristics of protection material (Light weight concrete)
    dp=0.020 ;             % dp = 20 mm
    rhop=1600;             % rhop = 1600 kg/m3
    Cp=840;               % Cp = 840 J/kg°K
    kp=0.8;               % kp = 0.8 W/m°K
    mc=0.05;               % mc = 5% (Moisture content)
   case 4,
% Characteristics of protection material (Brick with holes)
    dp=0.050;              % dp = 50 mm
    rhop=1000;             % rhop = 1000 kg/m3
    Cp=1200;               % Cp = 1700 J/kg°K
    kp=0.4;               % kp = 0.2 W/m°K

   otherwise
   return;
   %séquence d'instructions par défaut
end
 % Beam with circle Holes
D=0.714*h                  % Diameter of hole
rh=D/2 ;                   %  Radius of  hole
Ah=pi*rh^2 ;               % Area of a hole
Hp= 2*pi*rh ;              % Perimeter of a hole
%
%
boltz=5.67e-8;         % Stephan Boltzmann constant (=5,67×10-8 [W/m2K4])
%
% For Unprotected internal steelwork exposed in 4 sides
Am1=4*b+2*(h-tw-4*r)+2*pi*r; % for 4 sides
V=A;
AmV1=Am1/V; AmVb1=2*(h+b)/A;% for 4 sides
ksh1=0.9*AmVb1/AmV1; % for 4 sides

% For Unprotected internal steelwork exposed in 3 sides
Am2=3*b+2*(h-tw-4*r)+2*pi*r; % for 3 sides
```

```
V=A;
AmV2=Am2/V; AmVb2=(2*h+b)/A; % for 3 sides
ksh2=0.9*AmVb2/AmV2;        % for 3 sides

% For Protected internal steelwork in 4 sides
Ap1=2*(h+b);              % for 4 sides
V=A;
ApV1=Ap1/A;

% For Protected internal steelwork in 3 sides
Ap2=2*h+b;                % for 3 sides
V=A;
ApV2=Ap2/A;

% vector data
ksh_vect=[ksh1 ksh2];
AmV_vect=[AmV1 AmV2];
ApV_vect=[110 ApV2]

Dt=1;  % in seconds

tf=7201;

for j=1:length(ApV_vect)
   i=1;
   t=0;
   time(i)=t;
   Ta(i,j)=20;   Tg(i,j)=20;
   ksh=ksh_vect(j);
   AmV=AmV_vect(j);
   ApV=ApV_vect(j);
% Section of Steel exposed to fire on 4 and 3 sides and protected on 4 or 3
% sides
for i=2:tf
   t=t+Dt;
   time(i)=t;

   Ca=prop_ca(Ta(i-1,j));

   Tg(i,j)=20+345*log10(8*t/60+1);
   DTgt=Tg(i,j)-Tg(i-1,j);
     if DTgt<=0
        DTgt=0;
     end

   phit=(Cp*rhop)/(Ca*rhoa)*dp*ApV;
   DTat=(kp*ApV/(Ca*rhoa*dp)*(Tg(i,j)-Ta(i-1,j))/(1+phit/3))*Dt-(exp(phit/10)-1)*DTgt;
```

```
        if DTat<=0
        DTat=0;
      end
   Ta(i,j)=DTat+Ta(i-1,j);
end
end
%figure1=figure();
colors='gbkcmyr';
plot(time,Tg(:,1),'r','LineWidth',2)
for j=1:length(ApV_vect)
  hold on;
plot(time,Ta(:,j),colors(j),'LineWidth',2)
end
axis([0 tf 0 1000]);
xlabel('t [s]');
ylabel('T [°C]');
%title('Evolution of the temperature vs time (unprotected steel elements)')
title('PROTECTED SOLID BEAM ')
legend('ISO 834',namep1,namep2,'Location','northwest')
filename=strcat(namep,'.png');

set(gcf, 'PaperPositionMode', 'auto');
print('-dpng','-r200',filename)
%print(figure1,'-r300','-dpng',filename)
end

% material properties

function Ca=prop_ca(T);
 if and(T<600,T>=20)
      Ca=425+7.73e-1*T-1.69e-3*T^2+2.22e-6*T^3;
   elseif and (T<735,T>=600)
      Ca=666+13002/(738-T);
   elseif and (T<900,T>=735)
      Ca=545+17820/(T-731);
   elseif and (T<1200,T>=900)
      Ca=650;
   end;
end
```

Uncategorized References

[1]. Bailey, C., *Indicative fire tests to investigate the behaviour of cellular beams protected with intumescent coatings.* Fire Safety Journal, 2004. **39**(8): p. 689-709.

[2]. G. Bihina a, B.Z., A. Bouchaïr b, *Behaviour of composite steel–concrete cellular beams in fir.* (2013. **2217–2228**.

[3]. Wang, P., et al., *Web-post buckling of fully and partially protected cellular steel beams at elevated temperatures in a fire.* Thin-Walled Structures, 2016. **98, Part A**: p. 29-38.

[4]. Guo-Qiang Li a, J.H., n, Guo-Biao Lou a, Yong C. Wang, *Predicting intumescent coating protected steel temperature in fire using constant thermal conductivity.* Thin-Walled Structures, 2016. **177–184**.

[5]. Nadjai, A., et al., *Performance of unprotected and protected cellular beams in fire conditions.* Construction and Building Materials, 2016. **105**: p. 579-588.

[6]. Bailey, K.C.G., *Temperature distribution of intumescent coated steel framed connection at elevated temperature.* 2009. **8**(University of Manchester, UK): p. 8.

[7]. Bake, S., *Behaviour of cellular beams and cellular composite floors at ambient and elevated temperatures*, in *civil engenniring*. 2010, Manchester UK. p. 260.

[8]. Protection, A.f.S.F., *Fire protection for structural steel in buildings*. June 2004.: 2004. 162.

[9]. Delphine Sonck , J.B., *Lateral–torsional buckling resistance of cellular beams.* Journal of Constructional Steel Research, 2015. **105** p. 119–128.

[10]. Luis Mesquita, J.G., Gustavo Gonçalves, Paulo Piloto, Kada Abdelhak, *INTUMESCENT FIRE PROTECTION OF CELLULAR BEAMS.* 2015.

[11]. Jean-Marc Franssen, V.K., Raul Zaharia., *Designing Steel Structures for Fire Safety*. 2009. 158.

[12]. CEN, *EN1991-1-2 Eurocode 1: Actions on Structures, Part 1.2: General Actions, Actions on Structures Exposed to Fire.* 2002, European Committee for Standardization: Brussels, Belgium.

[13]. Wickstrom, U., *Comments on calculation of temperature in fireexposed bare steel structures in prEN 1993-1-2: Eurocode 3—design of steel structures—Part 1–2: general rules—structural fire design,Fire Safety Journal 40 .191-192, 2005*

[14]. Franssen, J.-M., *Calculation of temperature in fire-exposed bare steel structures:Comparison between ENV 1993-1-2 and EN 1993-1-2.* Fire Safety Journal 41, 2006: p. 139–143.

[15]. CEN, *ENV1993-1-2, Eurocode 3: Design of Steel Structures, Part 1-2: General rules, Structural fire design*. 1995, European Committee for Standardization: Brussels, Belgium.

[16]. *CEN, EN 13381-9: Test methods for determining the contribution to the fire resistance of structural members Part 9: Contribution of fire resistance to steel beams with web opening. 2015, European Committee for Standardization:*

. European Committee for Standardization?Brussels, Belgium., 2015.

[17]. *Test methods for determining the contribution to the fire resistance of structural members — Part 9: Applied fire protection systems to steel beams with web openings.* 2012(EN 13381-9:2012).

[18]. *CEN, EN1363-1: Fire resistance tests. General requirements.* . European Committee for Standardization: Brussels, Belgium., 1999,.

[19]. Chian, Y.M., *investigation on water-borne intumescent fire protective coatings for steel* 2011, MALAYA.

[20]. A. P. Mouritz, A.G.G., *Fire Properties of Polymer Composite Materials*. Vol. 143. 2006. 401.

[21]. *Test methods for determining the contribution to the fire resistance of structural members — Part 9: Applied fire protection systems to steel beams with web openings.* 2012.

[22]. *Test methods for determining the contribution to the fire resistance of structural members Part 8: Applied reactive protection to steel members*. april 2010: European Standart.